Summer 2011

Femtosecond laser micromachining of microstructures for sensing and detection

Yukun Han

Department: Mechanical and Aerospace Engineering

FEMTOSECOND LASER MICROMACHINING OF MICROSTRUCTURES FOR SENSING AND DETECTION

by

YUKUN HAN

A DISSERTATION

Presented to the Faculty of the Graduate School of the

MISSOURI UNIVERSITY OF SCIENCE AND TECHNOLOGY

In Partial Fulfillment of the Requirements for the Degree

DOCTOR OF PHILOSOPHY

in

MECHANICAL ENGINEERING

2011

Approved by

Hai-Lung Tsai, Advisor
Hai Xiao, Co-advisor
Darryl J. Alofs
K. Chandrashekhara
Xiaoping Du

PUBLICATION DISSERTATION OPTION

This dissertation has been prepared in the form of four papers for publication. Pages 5−17 have been published in Microsystem Technologies. Pages 17−31 have been published in Applied Physics A. Pages 31-46 have been published in Optical Engineering. Pages 46-60 have been published in Applied Physics A. All of them have been prepared in the format for publication in the corresponding journals. The balance of this dissertation follows the standard dissertation format.

ABSTRACT

This thesis focuses on the fabrication and analysis of miniature functional devices that can be used for different sensing and detection applications. As the first step, the surface characteristics and morphology of the micro/nano structures on substrates (fused silica and silicon) fabricated in water and in air by femtosecond laser were investigated. Based on this study, three micro devices have been designed and fabricated by femtosecond laser, and they were analyzed for optical and chemical sensing and detections. The three micro devices are: 1) an optical Fabry–Perot interferometer in optical fiber (made from fused silica) with smooth cavity surfaces. The Fabry–Perot interferometer was used to measure accurately the refractive index of solution and, hence, is capable of identifying different solutions; 2) a fused silica glass substrate for surface enhanced Raman spectroscopy (SERS). The optimized morphology (in nano/micron scales) on the fused silica surface with post chemical silver planting which can achieve a cross-section enhancement factor (EF) of 2.5×10^6, evaluated by 10^{-7} M Rhodamine 6G solutions; 3) a nanostructured silicon substrate for the surface-enhanced Raman scattering application. A simple and efficient method was developed to fabricate a substrate that was pre-coated with silver nitrite film to generate silver nanoparticles over a large–area. This study demonstrates that an EF greater than 5×10^5, measured by 10^{-6} M Rhodamine 6G solutions can be achieved. The proposed fabrication techniques and miniature devices can be used to integrate the SERS capability into a microchip (lab-on-a-chip) for biomedical and chemical analysis.

ACKNOWLEDGMENTS

I wish to express my sincere gratitude to my academic advisor, Dr. Hai-Lung Tsai, for providing guidance and constant encouragement during my graduate study at Missouri University of Science and Technology. He provided an excellent working atmosphere and supported me in every aspect. It has been a privilege and a pleasure to have worked with him. Also, I would like to thank my co-advisor Dr. Hai Xiao, Department of Electrical Engineering, for his valuable advices and kind help in my graduate research work.

I wish to extend my appreciation to Dr. Darryl J. Alofs, Dr. K. Chandrashekhara, and Dr. Xiaoping Du, for serving as committee members and for their examination of the dissertation.

The dissertation was supported in part by the Intelligent Systems Center at Missouri University of Science and Technology, which is gratefully acknowledged. Thanks are also due to the Department of Mechanical and Aerospace Engineering at Missouri University of Science and Technology for providing me a graduate teaching assistantship.

Lastly, I wish to thank my parents, my parents in law, my lovely baby girl Valery, and especially my husband, Zhi Liang, for their love, understanding, and support.

TABLE OF CONTENTS

LIST OF ILLUSTRATIONS

Figure Page

PAPER I

PAPER II

PAPER III

PAPER IV

LIST OF TABLES

1. INTRODUCTION

The latest advancement in femtosecond laser technology has opened a new window of opportunity for one-step fabrication of microdevices with true threedimensional (3D) configurations. Direct exposure of most solid materials (including fused silica glass and silicon) to ultra intense femtosecond laser pulses results in the quick establishment of free electron plasma at the focal point, leading to the ablation of a thin layer of materials. Femtosecond laser pulses with extremely high peak power produce almost no thermal damage as the pulse duration is shorter than the thermalization time. Femtosecond lasers have been successfully used for directly writing optical waveguides, micromachining microchannels and microchambers in glasses.

1.1 MINIATURIZED FIBER INLINE FABRY-PEROT INTEROMETER FOR HIGHLY SENSITIVE REFRACTIVE INDEX MEASUREMENT

Miniaturized and robust optical sensors capable of accurate and reliable measurement of refractive index of liquids have attracted tremendous interest in recent years due to their broad applications in chemical and biological sensing. Preferably, these devices shall have a small size, high sensitivity, fast response time and large dynamic range. Many existing devices operate based on evanescent field interactions. Examples include long period fiber gratings (LPFG) [1], chemically etch-eroded fiber Bragg gratings (FBG) [2], optical microresonators/ microcavities [3], fiber surface plasmon resonance (SPR) devices [4], photonic crystals [5], etc. In general, these devices have shown high sensitivity for refractive index measurement. Characterized as the resonance wavelength shift in response to refractive index changes, it has been reported that LPFGs can provide a sensitivity as high as 6000 nm/RIU (refractive index unit) while

microresonators can reach 800 nm/RIU [6]. However, the evanescent field-based devices have a nonlinear response to refractive index, meaning that the sensitivity varies at different refractive index ranges. The dynamic range of refractive index measurement is also limited. In addition, many existing devices have shown large temperature cross-sensitivity. As a result, temperature variation induced errors need to be corrected in real time.

Low finesse fiber Fabry-Perot interferometers (FPI) have been widely used as optical sensors for measurement of a variety of parameters such as pressure, strain, temperature, etc. [7]. However, they have been commonly made with a sealed cavity. [8-10] As a result, their applications have been mainly limited to the measurement of physical parameters. In a fiber FPI, the phase of the interference signal is linearly proportional to the optical length of the cavity, defined as the product of the cavity length and the refractive index of the medium filling the cavity. When exposed to the external environment, a FPI cavity can be used to measure the refractive index change with a linear response by tracking the phase shift of the interference signal. Compared with other types of sensors, a FPI refractive index sensor has the unique advantage of constant sensitivity over a large dynamic range. Xiao, et al., reported a FPI refractive index sensor formed by two polished fiber endfaces hosted in a holey sleeve [11]. The holey sleeve allows gas to freely enter and leave the cavity. However, the sensor assembly was complicated and required the use of epoxy and various components made of different materials. As a result, the device had a strong dependence on temperature. Recently, Ran, et al., described a refractive index sensor by adding a sealed Fabry-Perot cavity near the

tip of a single-mode fiber [12]. In this case, the sealed FPI itself was not a sensing device and only served as a signal modulator.

Recently, Rao, et al., reported a miniaturized fiber inline FPI device fabricated bymicromachining a rectangular non-through hole into a single-mode or photonic crystal fiber using a femtosecond laser [13]. The single-mode fiber FPI device had a fringe visibility of about 2 dB. Later, a 157 nm laser was used to improve the quality of abrication and a 26 dB fringe visibility was obtained using a photonic crystal fiber which had a strong absorption at the wavelength of 157 nm [14]. Assisted by the most recently developed femtosecond laser fabricated fiber inline FPI, the refractive index change can be calculated by the optical length change measured in fiber inline FPI. Since the fiber inline FPI was one step fabricated on the optical fiber, together with the fact that the refractive index measurement was carried out on the same device, the whole experiment was integrated on the same structure by one-time assembly, which further improved the measurement accuracy.

1.2 NANOSTRUCTURED FUSED SILICA AND SILICON SUBSTRATES WITH NANOPARTICLES FABRICATED BY FEMTOSECOND LASER FOR SURFACE-ENHANCED RAMAN SCATTERING

To achieve a high enhancement factor, many methods have been studied to fabricate high quality SERS substrates. SERS substrates are generally categorized into two main types, solid-phase patterned metallic nanoparticles or liquid-phase aggregated metallic nanoparticles from colloidal solutions. Solid phase based substrates have shown good stability and repeatability. SERS substrates can be made by direct physical deposition (e.g. sputtering and evaporation) of noble metals on to smooth surfaces. SERS substrates can also be made by roughening solid-state materials, including chemical

etching [15], silver particles hosted by porous silicon [16], bio-templated nanostructures [17], conventional lithography [18], etc.

Mazur's group reported a SERS substrate fabricated by machining nanostructures on an n-type silicon wafer using femtosecond laser pulse train with subsequent silver-deposition by thermal evaporation [19]. Cheng *et al*. wrote a waveguide-like micro-wire on Ag^{+} doped glass, and then grew the photo-reduced silver particles into a SERS suitable size by chemical plating [20]. A wild variety of optical devices (e.g. waveguides and resonators) can be integrated with SERS to further enhance the analysis capability. In 2007, Fan *et al*. demonstrated that an optical resonator could significantly enhance SERS signal through excitation laser multi-interaction with target molecules enabled by a tubular micro resonator [21].This may provide a way to integrate "finger print" SERS analysis into micro-fluidics system with one-step femtosecond laser micromachining. Fused silica glass substrates, well-known for their bio-compatibility and low cost, are one of the most competitive candidates for bioassay application. Silicon is the most common dielectric material in use. Femtosecond laser is one of the few flexible techniques for micro-machining silica glass substrates and silicon substrates with high accuracy and full controllability, offering a path to fabricate lab-on-a-chip and micro-total analysis system [20]. It is discussed that a fused silica glass-based SERS substrate fabricated by femtoseond laser and a simple method that can simultaneously fabricate nanostructures and generate silver nanoparticles by femtosecond laser pulses over a large area of the silicon substrate.

PAPER

I. Femtosecond laser-induced silicon surface morphology in water

Yukun Han[1], Cheng-Hsiang Lin[1], Hai Xiao[2] and Hai-Lung Tsai[1*]

1. Department of Mechanical and Aerospace Engineering 2. Department of Electrical and Computer Engineering

Missouri University of Science and Technology, Rolla, MO 65409

*Corresponding author: tsai@mst.edu

Abstract This article investigates the use of femtosecond laser induced surface morphology on silicon wafer surface in water confinement. Unlike irradiation of silicon surfaces in the air, there are no laser induced periodic structures, but irregular roughness is formed when the silicon wafer is ablated under water. The unique discovery of a smoothly processed silicon surface in water confinement under certain laser parameter combinations may help improve laser direct micromachining surface quality in industrial applications.

1. Introduction

Micro-structuring induced by using femtosecond (fs) laser has been widely discussed as appromising technique for total analysis system (μ-TAS) fabrication. The femtosecond laser direct-write process is controllable by programming and is highly efficient. Quite a few research groups have been investigating interesting phenomena-micro/nano scale periodic structures on some semiconductor materials. However, femtosecond induced micro/nano-scale periodic structures make the product surface too rough to be acceptable in the industrial world. Femtosecond laser direct-write sub-micron structures such as channels and resonators have been reported on transparent material like glass (Dong and Molian 2003; Hwang et al. 2004). Because these surfaces were still not acceptable, chemical etching was suggested as a methodology to decrease surface roughness (Dong et al. 2003). Although it works for specific kinds of materials in special solutions, it is not effective in every single case. Etching also lowers the fabrication efficiency. Thus, it is still worthwhile to look for a proper set of parameters for fabricating a smooth surface with a femtosecond laser. Especially for silicon, the most common dielectric material in use, the ultra-fast pulsed laser induced periodic structure is phenomenal, which makes it difficult to achieve a satisfactory surface after laser irradiation.

We will discuss some unique results of a laser direct-write experiment, which hold promise in the field of femtosecond laser application in silicon micro/nano-machining. With specific machining parameters, the machined surface on the silicon wafer has been smoothened strongly.

2. Experiment

The experiments were carried out at a home-integrated fs laser 3D micromachining system. The maximum repetition rate, center wavelength and pulse width of the fs laser (Legend-F, Coherent, Inc.) were 1 kHz, 800 nm and 80 fs, respectively. The maximum output power of the fs laser was approximately 1 W; however, we used a combination of a half-wave plate and a polarizer to first reduce the laser power to 20 mW, and then used several neutral density (ND) filters to further reduce the laser power to desirable values based on different experimental conditions. The attenuated laser beam was directed into objective lenses (Olympus UMPLFL 10X, 20X) with different numerical apertures (NA) and finally focused into the silicon samples. For fabrication of 3D microstructures, silicon samples were translated by a five-axis motion stage (Aerotech, Inc.) with a resolution of 1μm.

The fs laser was adjusted to focus on the silicon wafer sample. Trenches were fabricated layer by layer from the surface of the sample to inside of the sample. A 10X objective lens with NA = 0.30 was used in the processing.

As shown in Fig. 2, an empty liquid container is pre-loaded to the stage. The specimen was fixed to the bottom of the container so as to make it stable relative to the stage. Then, de-ionized water was added to the container to cover the surface of the specimen. Concerning the working distance of the objective lens, the depth of water should be less than 5 mm.

3. Results and discussions

We study on the effect of laser repetition rate on the ablated silicon surface quality. The repetition rate is adjustable from 1 to 1000 Hz. Six typical frequencies were selected in this experiment so as to fully elucidate the evolution of the surface patterns with the repetition rate, 500 Hz, 333 Hz, 250 Hz, 167 Hz, 100 Hz, and 10 Hz respectively. The traveling speed of the stage was set as 3mm/min and the pulse energy was fixed as of 0.2 μJ. The laser power is just above the ablation threshold. First, the experiments were taken in water confinement.

The machined surfaces after femtosecond laser scanning with different frequencies are shown in Fig. 3. All the images were taken at the same scale. The surface pattern after irradiation was found to vary significantly with the repetition rate when the scanning speed was fixed.

According to the above laser scanning results, a repetition rate of around 100 Hz, with pulse energy of 0.2 μJ, are good parameters for obtaining a smooth surface for application requirement. As the laser repetition rates increased, the surface became rougher. The roughness is due to big laser overlapping.

Next, by way of contrast, identical experiments were conducted in the air with the same series of parameters. It was found that the ablation threshold in air is the same as the ablation threshold in water. The phenomenal laser-induced periodic cones came into being, as shown in Fig. 4.

The potential mechanism of laser induced periodic structure formation in the air has been widely discussed. Some researchers indicated that oxidation might be a reason for the formation of nano-particles on the columnar spikes (Seifert et al. 2005), since the

content of dissociated oxygen is much higher than that in the water. The most widely accepted explanation takes into account the interaction of an electromagnetic wave with the microscopically rough selvedge of the surface. As the laser light hits onto the surface, the light may be refracted by the material, as well as scattered by the selvedge. The incoming laser light then interferes with the surface waves, leading to periodic electromagnetic field distribution. Hence, periodic structures form on the material surface (Georgescu, 2003).

The formation mechanism of surface pattern by laser direct writing in the water has seldom been studied. For underwater laser scanning, incident laser light interference with the surface waves is a possible reason for the boulder-furrow-like structure formation at frequencies of 167 Hz to 500 Hz. However, the morphology is not as regularly periodic as that obtained in the air. The water layer plays the role of shielding source from laser energy.

There are two possible causes of the special surface patterning phenomenon in water. First, as discussed previously, the cavitation bubbles caused by plasma formation and water evaporation significantly impact the interference processes. This might be a reasonable explanation for why the surface is corrugated, but not as regular as that in the air. Another reason is that H_2O molecules are strongly polarized due to the high electronegativity of the oxygen atoms. During the scanning process, the laser beam can be considered as a moving electromagnetic field on the sample surface. This moving electromagnetic field will affect the energy status of H_2O molecule because of its polarization. Then it influences the electromagnetic field itself in return. At an

appropriate laser pulse overlapping rate (changing with the change of the repetition rate), for instance, at 100 Hz, the surface quality will be improved a lot.

Then, we fabricate some structures on the silicon in water with the appropriate machining parameters we achieved to get a high quality machined surface. The results are shown in Fig. 5. Compared with the same structures machined in the air, the structure surface quality has been improved a lot. The periodic formation did not appear. The surface became much smoother.

4. Conclusion

In summary, we stated a femtosecond laser machining method to achieve clean, high quality surface on the silicon wafer under some specific laser machining parameters in the water confinement. It is unique way to avoid periodic structures that is induced by the femtosecond laser machining in the air on the machined silicon surface. It can help improve the silicon machining quality in many applications.

References

Dong Y., Molian P (2003) Femtosecond pulsed laser ablation of 3C-SiC thin film on silicon. Appl Phys A 77: 839-846. doi 10.1007/s00339-003-2103-y

Dong Y, Zorman C, Molian P. (2003) Femtosecond laser micromachining of single crystalline 3C-SiC structures based on a laser-induced defect-activation process. Journal of Micromech Microeng 13:680-685. doi: 10.1088/0960-1317/13/5/320

Georgescu I (2003) Pattern formation upon femtosecond laser ablation of transparent dielectrics. Diploma Thesis Brandenburgische Technische Universität Cottbus

Hwang, DJ, Choi, TY, Grigoropoulos CP. (2004) Liquid-assisted femtosecond laser drilling of straight and three-dimensional microchannels in glass. Appl Phys A 79: 605-612. doi 10.1007/s00339-004-2547-8

Seifert G, Kaempfe M, Syrowatka F, Harnagea C, Hesse D, Graener H (2005) Self-organized structure formation on the bottom of femtosecond laser ablation craters in glass. Appl Phys A 81: 799-803. doi 10.1007/s00339-004-2867-8

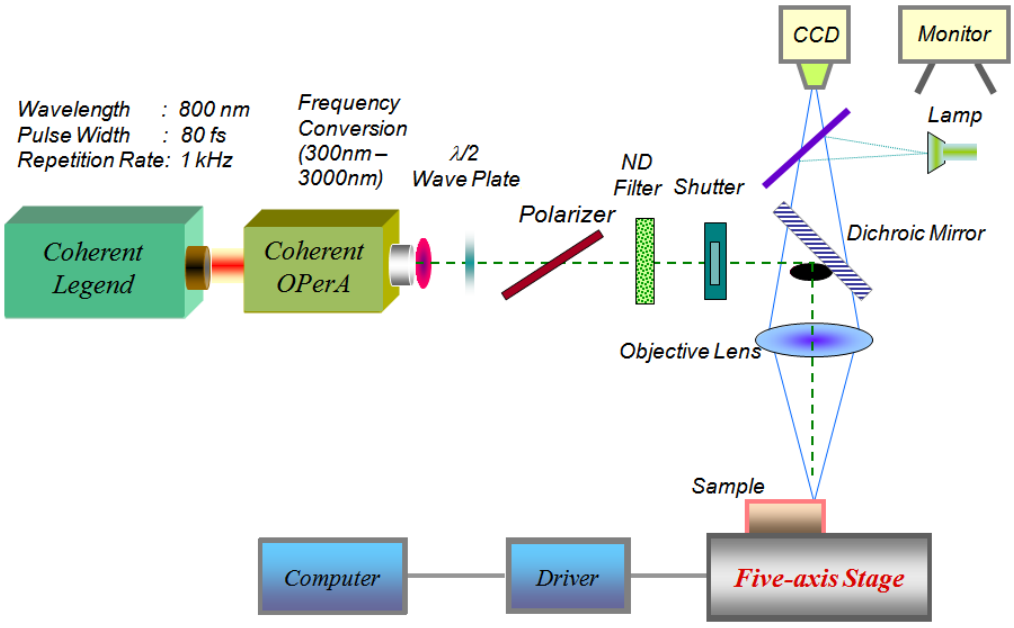

Fig.1 Schematic Diagram of experimental setup

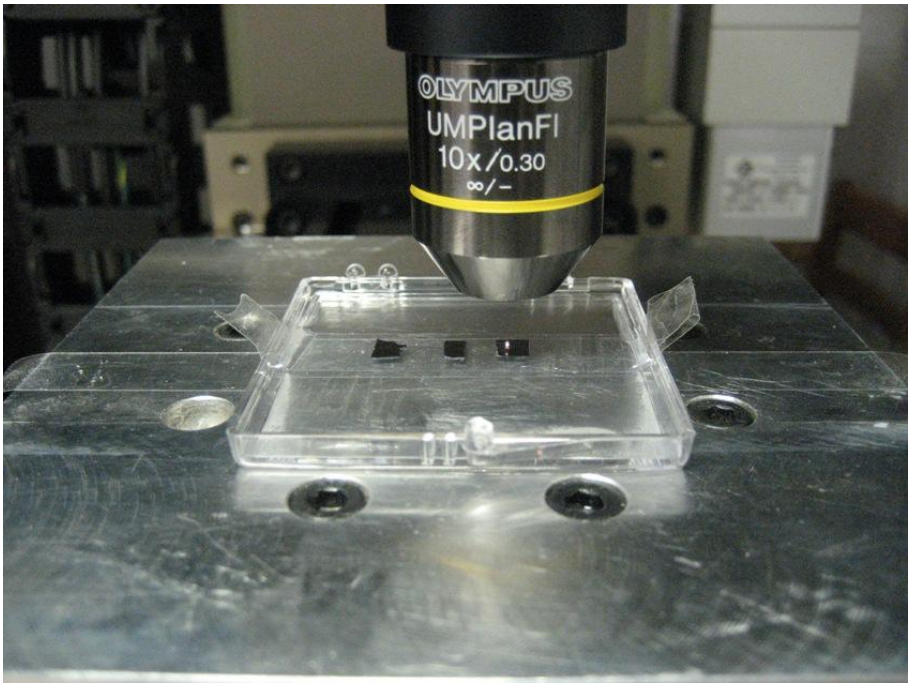

Fig.2 Specimen setup in water confinement

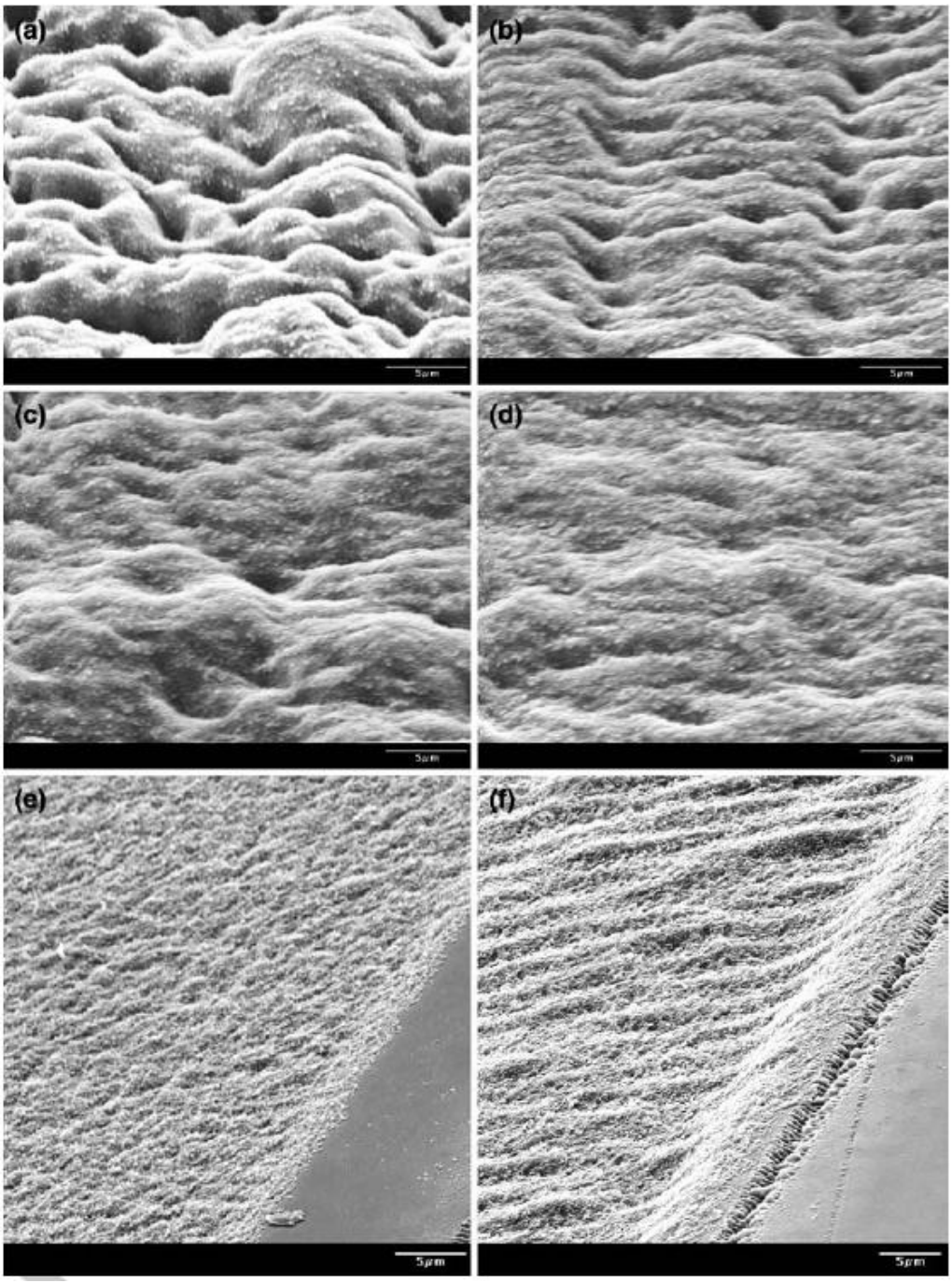

Fig.3 SEM images of femtosecond laser-induced surface morphology in water at (a) 500 Hz, (b) 333 Hz, (c) 250 Hz, (d) 167 Hz, (e) 100 Hz and (f) 10 Hz

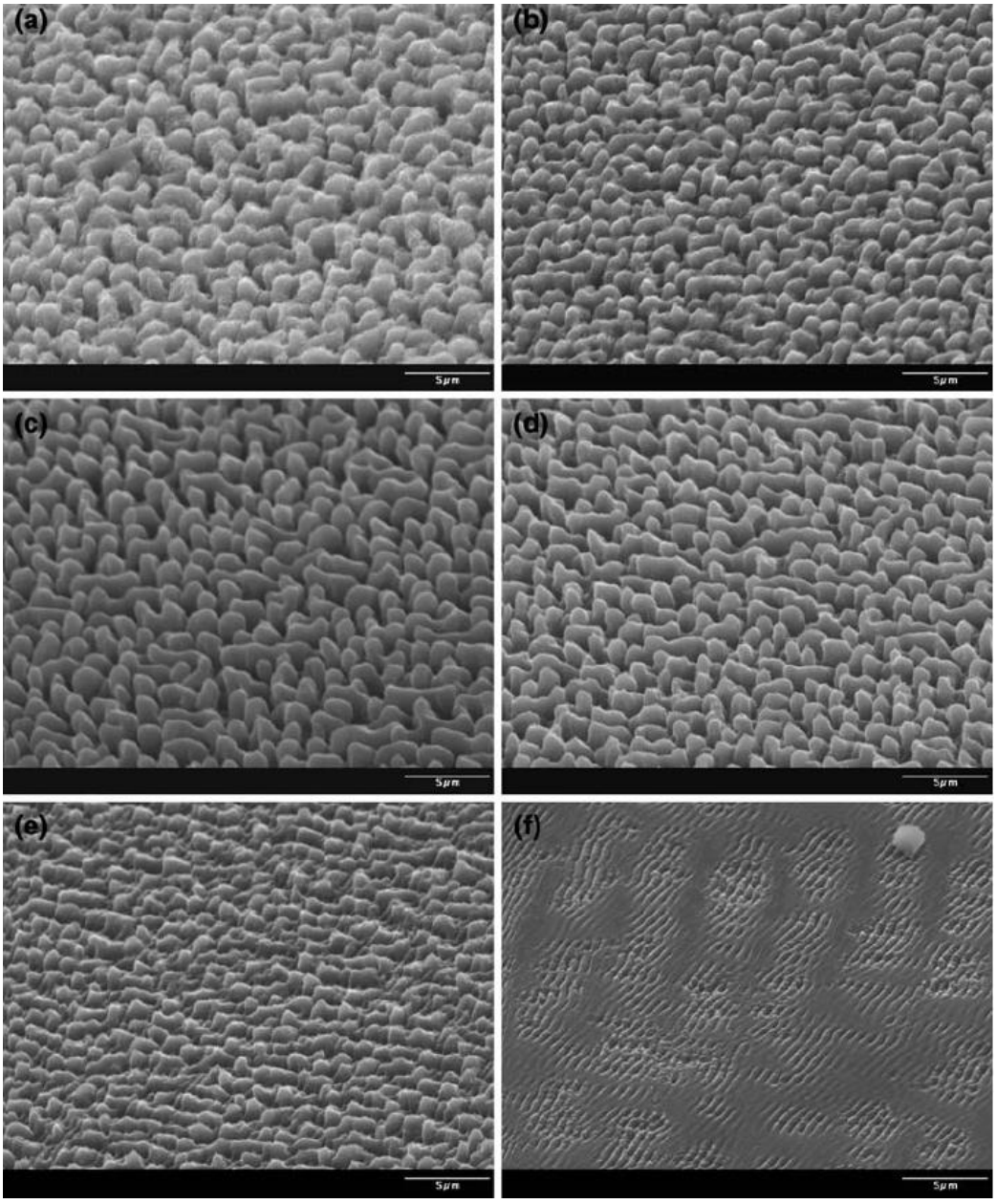

Fig. 4 SEM images of femtosecond laser-induced surface morphology in the air at (a) 500 Hz, (b) 333 Hz, (c) 250 Hz, (d) 167 Hz, (e) 100 Hz and (f) 10 Hz

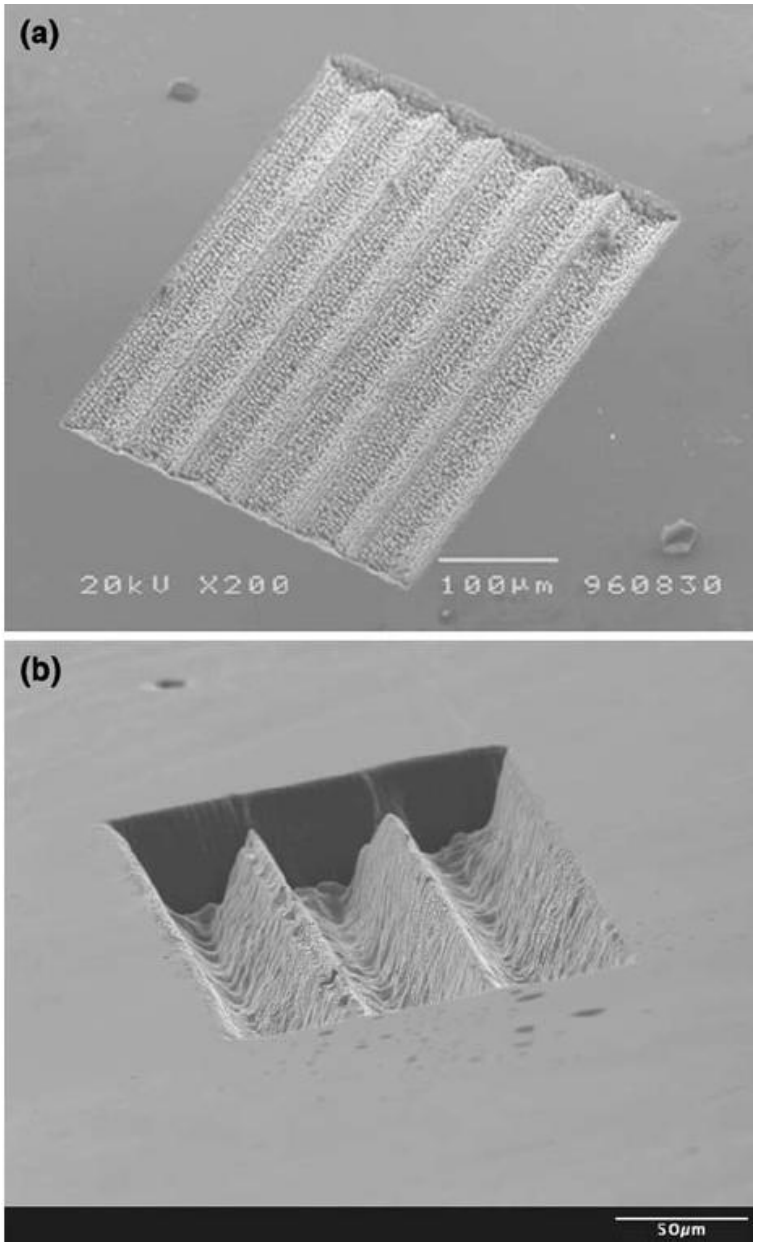

Fig. 5 V-shape grooves fabricated by fs laser direct writing in (a) air, and (b) water

II. Surface enhance Raman scattering silica substrate fast fabrication by femtosecond laser pulses

Yukun Han[1], Xinwei Lan[2], Tao Wei[2], Hai-Lung Tsai[1], Hai Xiao*[2]

[1]Department of Mechanical and Aerospace Engineering,

[2]Department of Electrical and Computer Engineering,

Missouri University of Science and Technology, 1870 Miner Circle, Rolla, MO 65409-0040, USA

*Corresponding author: xiaoha@mst.edu Fax: 01-573-341-4532 Tel: 01-573-341-6887

Abstract We report the fabrication of surface enhanced Raman spectroscopy (SERS) fused silica glass substrates using fast femtosecond (fs) laser scan, followed by silver chemical plating. A cross section enhancement factor (EF) of 2.5×10^6, evaluated by Rhodamine 6G (10^{-7} M solution), was obtained. The Raman mapping indicated a good uniformity over the fs laser scanned area. The dimension and pattern of the SERS activated region can be conveniently controlled by laser 2D scanning, potentially enabling integration of SERS into a high order optical-chemical analysis system on a glass chip.

PACS 61.80Ba · 42.65Re · 81.05Kf

1 Introduction

Since originally discovered in the 1970s [1,2], surface enhanced Raman scattering has been widely investigated. It was found that silver and gold nanosized particles could significantly enhance the Raman signal of molecule adsorbed onto the particle surface through the combined effects of electromagnetic and chemical enhancemnent. Enhancement factors (EF) as high as ~10^{14} on "hot spots" have been previously reported using Rhodamine 6G (R6G) as a probe molecule, showing the feasibility of single molecule detection [3].

To achieve a high EF, many methods have been studied to fabricate high quality SERS substrates. SERS substrates are generally categorized into two main types, solid-phase patterned metallic nanoparticles or liquid-phase aggregated metallic nanoparticles from colloidal solutions. Solid phase based substrates have shown good stability and repeatability. SERS substrates can be made by direct physical deposition (e.g. sputtering and evaporation) of noble metals on to smooth surfaces. SERS substrates can also be made by roughening solid-state materials, including chemical etching [4], silver particles hosted by porous silicon [5], bio-templated nanostructures [6], conventional lithography [7], etc.

The latest advancement in femtosecond (fs) laser technology has opened a new window of opportunity for one-step fabrication of nano/micro-devices with three-dimensional (3D) configurations. Direct exposure of most solid materials (include fused silica glass) to ultraintense fs laser pulses results in the quick establishment of free electron plasma at the focal point, leading to the ablation of a thin layer of materials [8]. Fs laser pulses with extremely high peak power produce nearly no thermal damage as the

pulse duration is shorter than the thermalization time. Due to the multiphoton nature of the interaction, the ablation process can be conducted on the material surface as well as within the bulk. Fs lasers have been successfully used for directly writing optical waveguides, and machining microchannels and microchambers in glasses [9].

Recently, Mazur group reported a SERS substrate fabricated by machining nanostructures on a n-type silicon wafer using fs laser pulse train with subsequent silver-deposition by thermal evaporation [10]. Cheng *et al*. wrote a waveguide-like micro-wire on Ag^{+} doped glass, and then grew the photo-reduced silver particles into a SERS suitable size by chemical plating [11] This may provide a way to integrate "finger print" SERS analysis into micro-fluidics system with one-step fs laser micromachining. Fused silica glass substrates, well-known for their bio-compatibility and low cost, are one of the most competitive candidates for bioassay application. A wild variety of optical devices (e.g. waveguides and resonators) can be integrated with SERS to further enhance the analysis capability In 2007, Fan *et al*. demonstrated that an optical resonator could significantly enhance SERS signal through excitation laser multi-interaction with target molecules enabled by a tubular micro resonator [12]. Fs laser is one of the few flexible techniques for micro-machining silica glass substrates with high accuracy and full controllability, offering a path to fabricate lab-on-a-chip and micro-total analysis system [11].

In this paper, we report a fused silica glass-based SERS substrate fabricated by fs laser. Using a fs laser scanning method to nanostructure a designated area on the glass substrate, followed by a silver chemical plating process, we obtained a high performance SERS substrate with a consistent EF of ~10^{6} covering the interacted area using R6G as

analyte molecule at the excitation wavelength of 632.8 nm. It is worth noting that chemical plating alone can make good quality SERS substrate on silica glass [13]. However, this process lacks the controllability of shape and dimension of the SERS-active area, causing it unsuitable to be further integrated into high-order systems.

2 Experiment

Laser nanostructuring SERS substrates were fabricated on fused silica glass using a home-integrated fs laser 3D micromachining system. The repetition rate, center wavelength and pulse width of the fs laser (Legend-F, Coherent, Inc.) were 1 kHz, 800 nm and 80 fs, respectively. The attenuated laser beam (0.7 nJ) was directed into an objective lens (Olympus UMPLFL 20×, NA 0.46) and focused onto the upper surface of silica glass slide mounted on a computer-controlled five-axis translation stage (Aerotech, Inc.). The computer controlled stage moved the sample at a speed of 1 mm/s, spacing the neighboring laser ablation points at a distance of 1 μm, considering a 1 kHz repetition rate. Upon finishing a line scan, the fiber was stepped transversely by 1μm to start another line scan. A 1500 μm ×100 μm rectangular substrate on the glass took about 5 min to complete.

Chemical plating Formation of silver nanoparticles on the laser scanned substrate proceeded as follows. The laser scanned substrate was clean carefully in an ultrasonic ethanol bath, rinsed with de-ionized water, and dried in a nitrogen environment. A container cleaned with concentrated H_2SO_4 was well rinsed using de-ionized water to hold the plating solution. The plating solution was prepared by mixing 30 ml of 0.3 M silver nitrate aqueous solution with 30 ml of 0.2 M NaOH to obtain a fine brown

precipitate of Ag_2O. A 0.4 M ammonia solution was then added into the mixture drop by drop until the precipitate completely dissolved to form $[Ag(NH_3)_2]^+$. A 0.3 M silver nitrate solution was added until the solution became pale brown. After 1 drop of 0.4 M ammonium was added, the solution became transparent again, and the dried glass substrate was then fully immersed into the solution. A 30 ml of 0.1 M α-lactose was then added into the solution to reduce the silver ions to form silver particles.

SERS measurement Characterization of pristine SERS substrates was carried out on a commercial Raman spectroscopy system (Horiba Jobin Yvon). A 632.8 nm HeNe laser was used to excite the Raman signal. Raman spectra were recorded through a 10x microscope objective (NA 0.25) and projected onto a charge-coupled device (CCD) array using a 1200 g/mm grating with an integration time of 5s.

3 Results and Discussion

Microscopic characterizations A single laser pulse ablated an area about 1.5 μm in diameter on the glass substrate as observed under scanning electron microscope (SEM). Figure 1(a) shows the field emission SEM image of the fs laser nanostructured silica glass substrate. Figure 1(b) and (c) show the top and side view SEM images of a laser ablated glass substrate after 5 min silver-deposition. The laser scanned silica surface exhibited a highly porous structure with hollow holes at a size of several hundred nanometers. The depth of the hole is about 700 nm estimated from the side view SEM image. We believe that the overlapping between two adjacent exposures created the nanometer scale roughness. The UV/VIS absorption spectrum of the silver coated laser ablated substrate was measured by a spectrometer (Cary 5 UV-VIS). As shown in Figure

2, the absorption maximum was found at 390 nm. The fs laser sculptured pores well accommodated chemically deposited silver particles on the order of 50-100 nm, which, we believe, created an appropriate metallic surface that accounted for the strong SERS signal.

SERS characterizations An aliquot of 3 μL R6G (10^{-7} M in distilled water) was dropped on the substrate. The dropped solution was spread evenly onto an area of about 3 mm in diameter. The estimated R6G molecular coverage on the substrate surface was 2.6×10^{12} molecules/cm^2. This was equal to about one molecule per 39 nm^2. In a densely packed R6G monolayer, a single molecule is supposed to take no more than 4 nm^2 in area [13, 14]. In our experiment, the R6G molecular coverage was low enough to exclude the formation of multi-layers. In other words, each dye molecule should directly interact with the substrate surface.

Using the bench-top Raman spectrometer, the Raman spectrum of a 5 min silver-coated substrate was measured as given in Figure 3. Trace (a) is the Raman spectrum of the R6G solution on a randomly chosen spot in the laser ablated area with the excitation laser power of 1.7 mW and integration time of 5 s. Trace (b) is the Raman signal of R6G solution of 10^{-3} M concentration measured on a laser ablated but uncoated glass substrate using the excitation laser power of 17 mW and integration time of 5 s. Comparison between these two traces indicates a strong Raman signal enhanced by the silver coated laser ablated glass substrate. According to reference [14, 15], Raman scattering cross-section EF for the substrate can be estimated by the following equation

$$EF = \frac{I_{SERS} N_{nR}}{I_{nR} N_{SERS}} \qquad (1)$$

where I_{nR} and I_{SERS} are the normal Raman and SERS intensities in the unit of $mW^{-1}sec^{-1}$ [16], respectively. N_{nR} and N_{SERS} represent the number of molecules probed in the reference sample and on the SERS substrate, respectively. Using the Raman peak at 610 cm^{-1} as the basis of calculation [17], the signal enhancement was estimated to be 2.5×10^6.

Raman mapping The uniformity of laser ablated SERS substrate was investigated by Raman mapping. Figure 4 shows the microscopic optical image and Raman mapping of a T-shape SERS activated region (250 μm×150 μm). The mapping was taken as the Raman intensity integrated in the range from 700 to 1800 cm^{-1}. The excitation laser power was 1.7 mW; the integration time was 2 s; the microscopic lens was a 10× objective (NA=0.25); the spatial scanning step was 10 μm. The inset of Fig. 4 shows the optical microscopic image of the T shape area, where the width of the laser structured area was 50 μm. The Raman signal distribution shows a good homogeneity over the laser ablated area, while the non-structured area has no observable Raman signal. It is worth noting that the intact region was also deposited by silver particles during the same chemical plating process. However, the coated silver layer alone did not have a significant contribution to the SERS enhancement, compared to the laser ablated area. We believe it is the combination of porous surface fabricated by fs laser and silver coating that accounts for the strong SERS signal.

4 Conclusion

To summarize, a SERS substrate fabricated by fs laser ablation on a silica glass, followed by chemical plating of silver, was demonstrated. An EF of 2.5×10^6 was measured using a 10^{-7} M R6G solution. Besides the high EF, the fs laser structured area has shown a good

uniformity characterized by Raman mapping. Fs laser technique could be potentially used to fabricate SERS regions with a controlled dimension and arbitrary pattern by fast and convenient laser 2D scanning, enabling integration of SERS into high order optical system on a single glass chip.

Acknowledgment The research work was supported by the Office of Naval Research through the Young Investigator Program (N00014-07-0008) and the University of Missouri Research Board (UMRB).

References

1. M. Fleischmann, P. J. Hendra, A. J. Mcquillan, Chem. Phys. Lett. **26**, 163 (1974)
2. D. L. Jeanmaire, R. P. Van Duyne, J. Electroanal. Chem. Interf. Electrochem. **84**, 1 (1977)
3. S. M. Nie, S. R. Emery, Science, **275**, 1102 (1997)
4. S. Chan, S. Kwon, T. W. Koo, L. P. Lee, A. A. Berlin, Adv. Mater. **15**, 1595 (2003)
5. W. Yan, L. Bao, S. M. Mahurin, and S. Dai, Appl. Spectrosc. **58**, 18 (2004)
6. G. Kostovski, D.J. Whiteb, A. Mitchell, M.W. Austin, P.R. Stoddart, Biosensors and Bioelectronics, **24**, 1531 (2009)
7. M. Kahl, E. Voges, S. Kostrewa, C. Viets, W. Hill, Sensors and Actuators B, **51**, 285 (1998)
8. K. M. Davis, K. Miura, N. Sugimoto, and K. Hirao, Opt. Lett. **21**, 1729 (1996).
9. A. Szameit, D. Bloemer, J. Burghoff, T. Pertsch, S. Nolte, F. Lederer, and A. Tuennermann, Appl. Phys. B, **82**, 507 (2006).
10. E. D. Diebold, N. H. Mack, S. K. Doorn, E. Mazur, Langmuir, **25**, 1790 (2009)
11. Z. Zhou, J. Xu, Y. Cheng, Z. Xu, Jpn. J. Appl. Phys. **47**, 189 (2008)
12. I. M. White, J. Gohring, and X. Fan, Opt. Express, **15**, 17433 (2007)
13. M. Baia, L. Baia S. Astilean and J. Poop, Appl. Phys. Let. **88** 143121 (2006)
14. A. Kudelski, Chem. Phys. Lett. **414** 271 (2005)
15. H. K. Park, J. K. Yoon, K. Kim, Langmuir, **22**, 1626 (2006)
16. R.P. Van Duyne, J. C. Hulteen, and D. A. Treichel, J. Chem. Phys. **99** 2101 (1993)
17. S. Santesson, J. Johansson, L. S. Taylor, I. Levander, S. Fox, M. Sepaniak, and S. Nilsson, **75**, 2177 (2003)

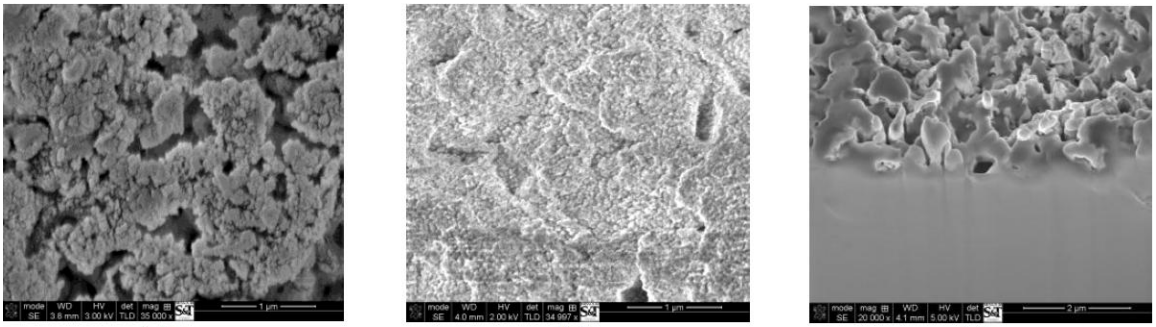

Fig. 1 SEM images of fs laser fabricated SERS silica glass substrates, (a) nanostructured substrate before chemical plating, (b) top view of a 5 min silver chemically plated substrate, and (c) side view of a 5 min silver chemically plated substrate

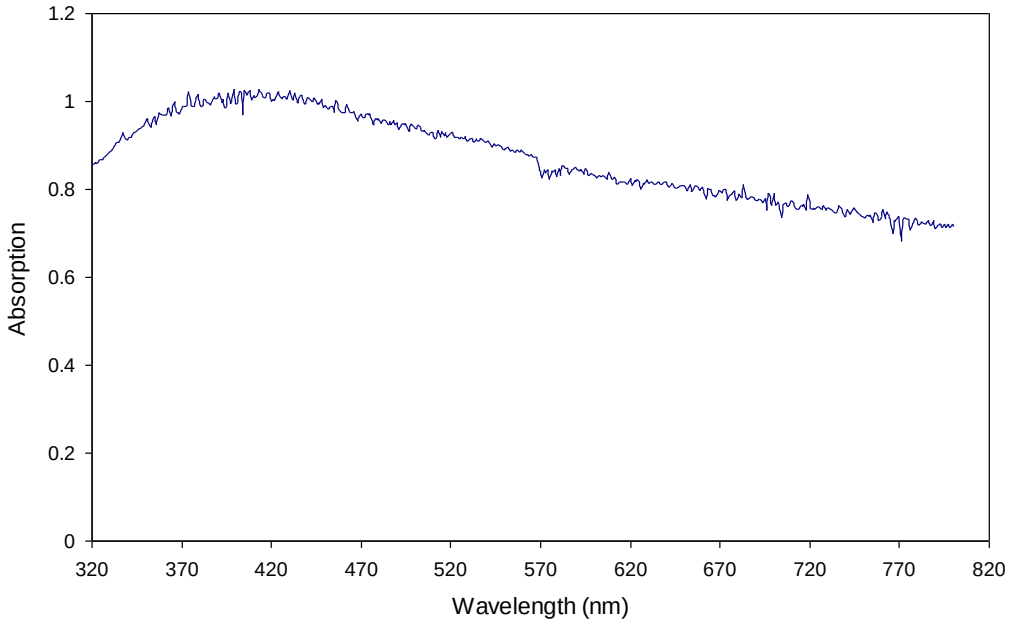

Fig. 2 UV/VIS absorption spectrum of a silver-coated, fs laser ablated SERS glass substrate

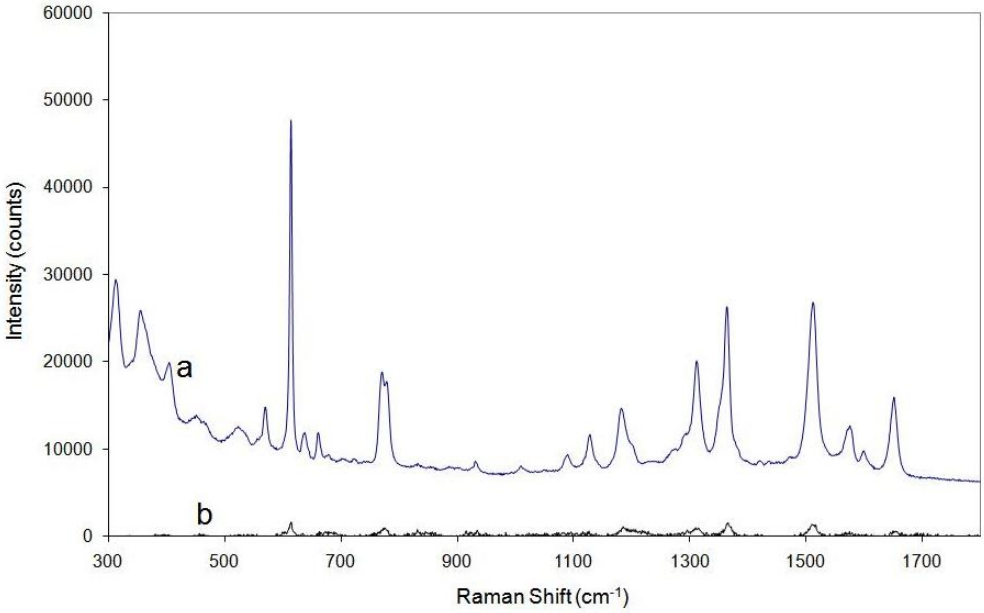

Fig. 3 Raman spectra of R6G. (a) Raman spectrum of R6G 10^{-7} M solution dispersed on the silver-coated, laser ablated SERS substrate with an excitation laser power of 1.7 mW and integrated time of 5 s, and (b) Raman spectrum of R6G 10^{-3} M solution on the laser ablated but non-silver-coated glass substrate with an excitation power of 17 mW and integrated time of 5 s

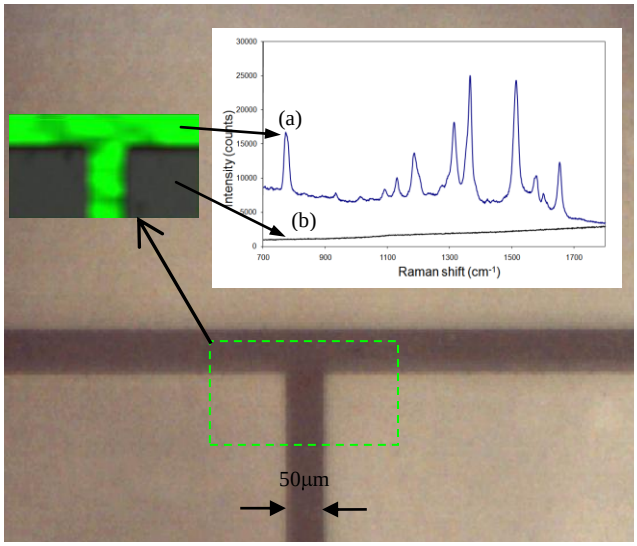

Fig. 4 Microscopic image and Raman mapping of a T-shaped SERS area fabricated by fs laser ablation followed by 5 min silver chemical plating, (a) Raman spectrum of R6G solution in the laser structured area, and (b) Raman spectrum of R6G solution in the non-structured area

III. Measurement of refractive index change of optical fiber core induced by femtosecond laser scanning

Yukun Han[1], Tao Wei[2], Hai-Lung Tsai[1]* and Hai Xiao[2]

[1]Department of Mechanical and Aerospace Engineering,

[2]Department of Electrical and Computer Engineering,

Missouri University of Science and Technology, 1870 Miner Circle, Rolla, MO 65409 USA

*Corresponding author: tsai@mst.edu

Abstract. We report a new method to measure the refractive index change in optical fiber core induced by femtosecond (fs) laser exposure. An in-line Fabry-Perot interferometer, serving as the measurement platform, was constructed on a commercial single mode optical fiber by one-step femtosecond (fs) laser fabrication. A positive refractive index change was observed and measured accurately as the laser pulse energy surpassed the ablation threshold.

Subject terms: femtosecond laser; refractive index; optical fiber; Fabry-Perot Interferometer.

1 Introduction

Recent advancement in ultrafast (~femtosecond) pulse laser technology has opened a new window of opportunity for one-step (without additional assembly) fabrication of micro- and even nano-scale photonic structures in various solid materials.[1,2] A fs laser beam can be focused into a transparent object, creating localized optical features at the focal point on the surface or inside the solid material. Various miniaturized optical devices have been demonstrated using fs lasers. Compared with other fabrication methods, fs laser-based technique has the unique feature of fabricating three dimensional (3D) microstructures with great flexibility.

Femtosecond-laser-based fabrication of optical devices can be either destructuive or non-destructive. In a destructive fabrication, the fs laser ablation effect is directly used to sculpture solid materials into desired 3D shapes. Optical device examples include microlenses,[3] microfluidic channels,[4] fiber inline Fabry-Perot interferometers,[5-6] and optical switches.[7] Destructive fabrication is above the material ablation threshold. Nondestructive fabrication named sub-ablation fabrication is blow the material ablation threshold. Although the point at which absorbed laser energy is not sufficient to break the bonds between molecules of a material, the short-pulse lasers causes near-surface thermal stresses, which can lead to a wide variety of micromechanical responses.[8-9] In a nondestructive way, fs laser irradiations can induce refractive index in optical materials.[10-12] As a result, optical waveguides,[13-14] gratings,[15-16] and directional couplers[17] have been demonstrated, for instance, fiber bragg gratings and long period fiber bragg gratings. The amount of refractive index variation induced by fs laser exposure inside the photonic device is one of the most critical variables that determine the characteristic of the target structure, such as fiber bragg grating. Quite a few research groups study on

laser induced refractive index change in different materials. However, up to date, although the fs laser induced refractive index change on bulk fused silicon has been studied, no precise measurement was conducted towards this parameter in optical fiber.

This work mainly focuses on the measurement method of fs laser induced refractive index change in optical fiber core. Assisted by the most recently developed fs laser fabricated fiber inline FPI, the refractive index change can be calculated by the optical length change measured in fiber inline FPI. Since the fiber inline FPI was one step fabricated on the optical fiber, together with the fact that the refractive index measurement was carried out on the same device, the whole experiment was integrated on the same structure by one-time assembly, which further improved the measurement accuracy.

2 Measurement Platform Fabrication

Figure 1 shows the optical image of the fabricated fiber inline FPI (Fabry-Perot interferometer) device. The device was fabricated out for an optical fiber (Corning SMF-28) by fs laser micromachining following the procedures reported previously.[5] The cavity length was about 40 μm as estimated from the optical image. The depth of micro-notch was around 72 μm, just passing the fiber core. The cavity was made 5 mm to the end of the cleaved fiber tip. The background loss of this particular device was about 20 dB. This device can be concerned as a combination of two FPIs. The fs laser ablated notch section is the extrinsic Fabry-Perot interferometer (EFPI), while the following fiber segment to the end of the fiber tip is the intrinsic Fabry-Perot interferometer (IFPI). The EFPI corresponds to interference spectra with a period of around 40 nm, and the IFPI has that

of around 0.15 nm. In this experiment, the IFPI was used as the measuring device and the IFPI signal is relatively independent from that of EFPI as a result of the huge scale difference between the interference spectra. With femtosecond laser scanning close to IFPI cavity, the shift of IFPI interference can be detected due to the refractive index change in the fiber core.

3 Principle and Theory

The refractive change can be measured using a fiber inline FPI as schematically shown in Fig. 2. The IFPI section serves as an interferometer, in which the reflections at the two endfaces, coupling back to the lead in fiber through the fs ablated notch (EFPI section), superimposed to form an interference signal at the optical power meter (HP8163). By stepping the tunable laser through its available wavelength range and coordinating the signal detection at the power meter using a computer, the interference spectrum of the IFPI can thus be recorded. When exposed to fs laser irradiations, the IFFPI section at the end of the fiber tip changes its refractive index, resulting in a phase shift in the interference signal. The fs laser induced fiber refractive index change can thus be calculated based on the amount of phase shift after laser irradiation.

Assuming that the two reflected lights from the IFPI section have the intensities of I_1 and I_2, respectively, the interference signal I_i generated by these two reflections is given by reference 6:

$$I_i = I_1 + I_2 + 2\sqrt{I_1 I_2}\cos(\frac{4\pi}{\lambda}(OL) + \phi_0) \quad (1)$$

where *OL* is the optical length of IFPI, defined as the product of length and the refractive index of the core; Φ_0 is the initial phase of the interference; λ is the optical wavelength in vacuum.

As shown in Fig. 2, the two adjacent valleys at λ_1 and λ_2 in the interference spectrum have a phase difference of 2π, that is:

$$(\frac{4\pi}{\lambda_1}OL)-(\frac{4\pi}{\lambda_2}OL)=2\pi \tag{2}$$

Therefore, the initial optical length of the IFPI section can be calculated using the following equation:

$$OL=\frac{\lambda_1\lambda_2}{2(\lambda_1-\lambda_2)} \tag{3}$$

Since the device is fixed under a tension free circumstance and the IFFPI section is considerably short (~5 mm), the change in optical length is mainly caused by the laser irradiation induced refractive index change inside the fiber core. For multiple-point laser irradiations at different locations, the accumulated change in optical path (ΔOL) is given by

$$\Delta OL=m\cdot(\Delta OL_{\text{single}})=m\cdot(\Delta n\cdot W) \tag{4}$$

where m is the total number of laser irradiations; Δn is the refractive index change and W is the width of one fs laser exposure scan.

When the change in optical path length is small so that the phase shift is less than 2π, the phase ambiguity issue can be avoided. The relative optical length change can be calculated based on the spectral shift of the interferogram at the featured points such as the peak, valley and the center of the interference fringes, given by reference 6

$$\Delta OL = \frac{\Delta\lambda_1}{\lambda_1} OL \tag{5}$$

Combining Eqs. (4) and (5), one finds the refractive index change:

$$\Delta n = \frac{1}{mW} \frac{\Delta\lambda_1}{\lambda_1} OL \tag{6}$$

In the experiments, the laser pulse energy was tunable. The laser pulse length (width) which is equal to the pulse wavelength was fixed. An alternative way of calculating the refractive index change is directly based on Eq. (4) in which the change in optical length is a linear function of the number of laser exposures and the slope of the line is linearly proportional to Δn. Experimentally, one can measure the optical length change after a various number of laser exposures and curve-fit the measurement results into a line. The slope of the fitted line can thus be used to calculate Δn. This method uses multiple data points in calculation and can effectively reduce the measurement uncertainty.

4 Experiment

The experiment was carried out at a home-integrated fs laser 3D micromachining. The repetition rate, center wavelength and pulse width of the fs laser (Legend-F, Coherent, Inc.) were 1 kHz, 800 nm and 80 fs, respectively. The maximum output power of the fs laser was approximately 1 W; A combination of a half-wave plate and a polarizer was used to reduce the laser power to 20 mW at the first place, and then several neutral density (ND) filters was applied to further reduce the laser pulse energy to desired values, 0.5 μJ, 0.8 μJ and 1 μJ, based on different experimental conditions. The attenuated laser beam was directed into objective lenses (Olympus UMPLFL 20X) with a numerical

aperture (NA) of 0.45 and was focused at the center of IFPI section. Each time, with the help of a five-axis motion stage (Aerotech, Inc.) providing 1 μm resolution, a block (20 μm ×15 μm ×15 μm) was scanned covering the fiber core potion with a width of 20 μm, defined as one fs laser exposure scan. We altered the distance between the single laser scans, as the experiment goes along, to avoid the grating effect, which might disturb the interference signal.

5 Results and Discussion

Figure 3 shows the initial interference spectrum and those after 10, 20 and 30 fs laser scans with laser pulse energy of 0.8 μJ. The large fringe visibility-the ratio of the size or amplitude of oscillations to the sum of the powers of the individual waves, indicated high-quality of the interference signals. Since each laser scan induced a small amount of energy loss, the fringe visibility of the interference signal reduced as the number of laser exposures increased. This is still an open topic; some groups employed the Kramers-Kronig relations to explain laser pulse properties and refractive index change.[18-19]

The interference spectrum shifts to the short wavelength as the number of laser scans increases. By tracing the interferogram shift, we calculated the changes of optical length based on Eq. (4). The results, as a function of the number of laser scans, are plotted in Fig. 4, where the measured data points fit nicely into a line with a slope of 6.9 nm per fs laser scan. The induced Δn was 3.45×10^{-4} based on Eq. (4).

To investigate the induced refractive index at alternative laser pulse energy, we repeated the above experiments by varying fs laser pulse energy though adding or dropping ND filters. Fig. 4 shows the change in fiber optical length as a function of the

number of the laser scans with different pulse energy of 0.5 μJ, 0.6 μJ, 0.8 μJ and 1 μJ. As for comparison, the refractive changes induced by different pulse energy are 2.5×10^{-6}, 2.78×10^{-5}, 3.45×10^{-4} and 8.95×10^{-4}, respectively. Obviously, the refractive index change induced by 0.5 μJ, approximately the refractive index modification threshold for fusion silicon ablation, is ignorable. The experiment revealed that pulse energy less than refractive index modification threshold cannot produce observable refractive index change, which we believe is due to the reason that smaller pulse energy below the threshold is not able to significantly change the material thermal stresses, inducing refractive index modification. Still, it is an open issue that remains further verification and investigation.

6 Conclusion

We demonstrated a fiber inline IFPI-based measurement method to investigate the fs laser induced refractive index change in optical fiber core. The fs laser induced refractive index change was found out as 2.5×10^{-6}, 2.78×10^{-5}, 3.45×10^{-4} and 8.95×10^{-4} at different pulse energy levels, 0.5 μJ, 0.6 μJ, 0.8 μJ and 1 μJ, respectively. We believe accurate refractive index change values can help develop and design non-destructive fs laser fabricated photonic device.

Acknowledgement

The research work was supported by the U.S. Department of Energy under Contract No. DE-FE0001127.

References

1. R.R. Gattass and E. Mazur, 'Femtosecond laser micromachining in transparent materials,' *Nature Photonics*, **2**(4), 219-225 (2008)
2. M. Lenzner, J. Krüger, S. Sartania, Z. Cheng, C. Spielmann, G. Mourou, W. Kautek, F. Krausz, "Femtosecond optical breakdown in dielectrics," *Phys. Rev. Lett*., **80**(18), 4076-4079 (1998)
3. Y. Cheng, H.L. Tsai, K. Sugioka, K. Midorikawa, "Fabrication of 3D microoptical lenses in photosensitive glass using femtosecond laser micromachining*," Appl. Phys. A.,* **85**(1), 11-14 (2006)
4. Y. Cheng, K. Sugioka, and K. Midorikawa, "Microfluidic laser embedded in glass by three-dimensional femtosecond laser microprocessing," *Opt. Lett.,* **29**(17), 2007-2009 (2004)
5. T. Wei, Y. Han, H-L. Tsai, and H. Xiao, "Miniaturized fiber inline Fabry–Perot interferometer fabricated with a femtosecond laser", *Opt. Lett.*, **33**(6), 536-538 (2008)
6. T. Wei, Y. Li, Y. Han, H-L. Tsai, and H. Xiao, "Temperature-insensitive miniaturized fiber inline Fabry-Perot interferometer for highly sensitive refractive index measurement", *Opt. Express*, **16**(8), 5764-5769 (2008)
7. H.Y. Zheng, H. Liu, S. Wan, G.C. Lim, S. Nikumb Q. Chen, "Ultrashort pulse laser micromachined microchannels and their application in an optical switch," *Int. J. Adv. Manuf. Technol*., **27**(9-10), 925-929 (2006)
8. J. Kruger, H. Niino and A. Yabe, "Investigation of excimer laser ablation threshold of polymers using a microphone', *Appl. Surf.*, **197-198**, 800-804 (2002)
9. A. Baum, P. Scully, M. Basanta, C. Thomas, P. Fielden and N. Goddard, "Photochemistry of refractive index structures in poly (methyl methacrylate) by femtosecond laser irradiation", *Opt. Lett.*, **32**(2), 190-192 (2007)
10. M. Kamata, and M. Obara, "Control of the refractive index change in fused silica glasses induced by a loosely focused femtosecond laser", *Appl. Phys.*, **78**(1), 85-88 (2004)
11. F. Vega, J. Armengol, V. Diez-Blanco, J. Siegel, J. Solis, B. Barcones, A. Pérez-Rodríguez, and P. Loza-Alvarez, "Mechanisms of refractive index modification during femtosecond laser writing of waveguides in alkaline lead-oxide silicate glass", *App. Phys. Lett.*, **87**(2), 1-3 (2005)
12. A. Zoubir, M. Richardson, L. Canioni, A. Brocas, and L. Sarger, "Optical properties of infrared femtosecond laser-modified fused silica and application to waveguide fabrication", *J. Opt. Soc. Am. B*, **22**(10), 2138-2143 (2005)
13. K. M. Davis, K. Miura, N. Sugimoto, and K. Hirao, "Writing waveguides in glass with a femtosecond laser," *Opt. Lett.*, **21**(21), 1729-1731 (1996)
14. S. Nolte, M. Will, J. Burghoff, and A. Tuennermann, "Femtosecond waveguide writing: a new avenue to three-dimensional integrated optics," *Appl. Phys A*, **77**(1), 109-111 (2003)
15. A. Martinez, M. Dubov, I. Khrushchev, and I. Bennion, "Direct writing of fiber Bragg gratings by femtosecond laser", *Elec. Lett.*, **40**(19), 1170-1172 (2004)

16. Y. Kondo, K. Nouchi, T. Mitsuyu, M. Watanabe, P. G. Kazansky and K. Hirao, "Fabrication of long-period fiber gratings by focused irradiation of infrared femtosecond laser pulses" *Opt. Lett.*, **24** (10) 646-648 (1999)
17. A. M. Streltsov, and N. F. Borrelli, "Fabrication and analysis of a directional coupler written in glass by nanojoule femtosecond laser pulses," *Opt. Lett*., **26**(1), 42-43 (2001)
18. K. Peiponen, V. Lucarini, E. Vartiainen, and J. Saarinen, "Kramers-Kronig relations and sum rules of negative refractive index media*", Eru. Phys.* **41**, 61-65 (2004)
19. H. Nishiyama, J. Nishii, M. Mizoshiri, and Y. Hirata, " Microlens arrays of high-refractive-index glass fabricated by femtosecond laser lithograpy", *Appl. Surf.* **255**, 9750-9753 (2009)

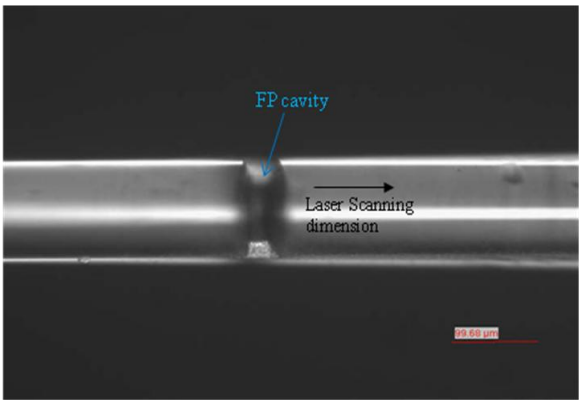

Fig. 1 The optical image of the fabricated fiber inline FPI device.

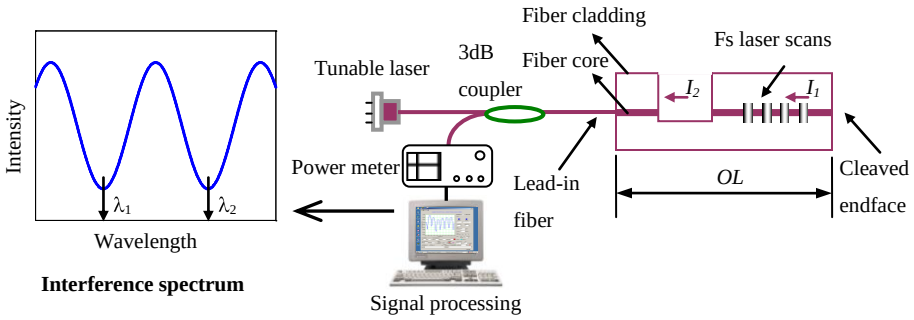

Fig. 2 The schematic of refractive change detection using a fiber inline FPI.

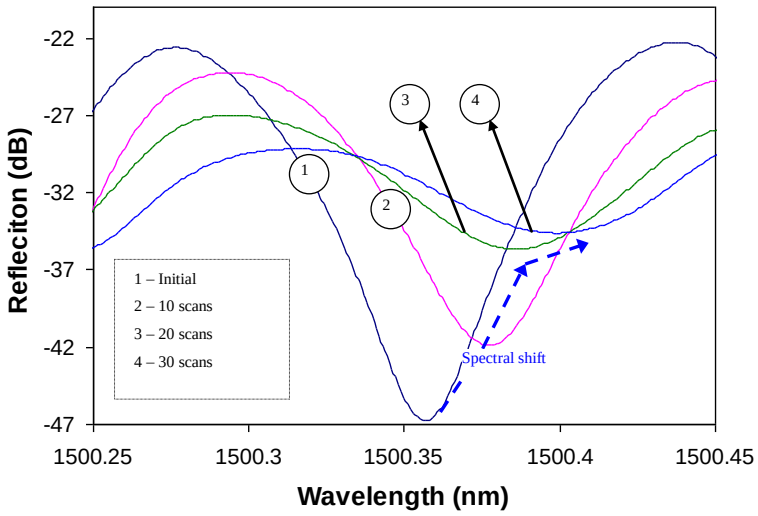

Fig. 3 The initial interference spectrum.

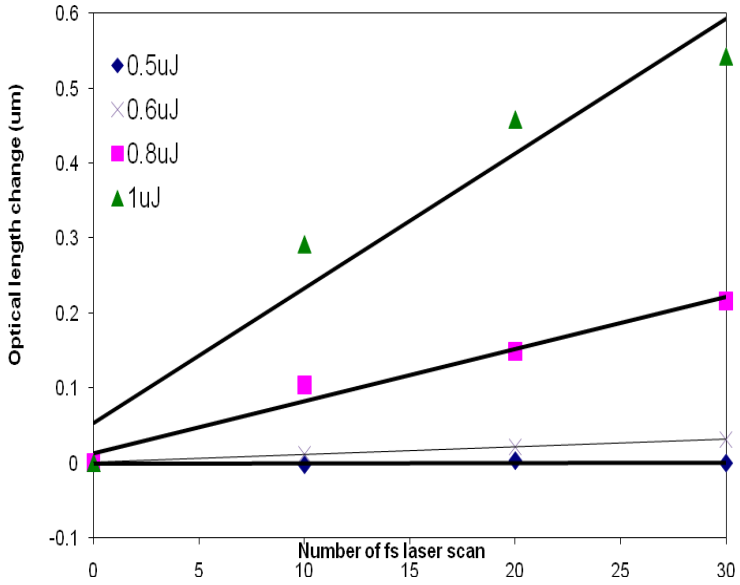

Fig. 4 The change in fiber optical length versus numbers of the laser scans.

IV. Nanostructured substrate with nanoparticles fabricated by femtosecond laser for surface-enhanced Raman scattering

Yukun Han,[1] Zhi Liang[1], Huilai Sun,[1, 2] Hai Xiao,[3] and Hai-Lung Tsai[1,*]

[1]Department of Mechanical and Aerospace Engineering, Missouri University of Science and Technology, Rolla, MO 65409, USA

[2]School of Mechanical and Electronic Engineering, Tianjin Polytechnic University, Tianjin, 300160 China

[3]Department of Electrical and Computer Engineering, Missouri University of Science and Technology, Rolla, MO 65409, USA

[*]Corresponding author: tsai@mst.edu

Abstract A simple and fast method to fabricate nanostructured substrates with silver nanoparticles over a large area for surface-enhanced Raman scattering (SERS) is reported. The method involves two steps: 1) dip the substrate into a silver nitrate solution for a few minutes, remove the substrate from the solution, and then air dry and 2) process the silver nitrate coated substrate by femtosecond (fs) laser pulses in air. The second step can create silver nanoparticles distributed on the nanostructured surface of the substrate by the photoreduction of fs multiphoton effects. This study demonstrates that an enhancement factor (EF) greater than 5×10^5, measured by 10^{-6} M Rhodamine 6G solution, can be achieved. The proposed technique can be used to integrate the SERS capability into a microchip for biomedical and chemical analysis.

PACS 61.80Ba · 42.65Re · 81.05.Cy

1 Introduction

Since the 1970s, the phenomena of surface-enhanced Raman scattering (SERS) by molecules adsorbed on a roughened metal surface have been widely investigated [1, 2]. The enhancement factor (EF) can be as high as 10^{14}–10^{15} using Rhodamine 6G (R6G) which allows the technique to be sensitive enough to detect a single molecule on a rough noble metal (e.g., silver and gold) surface [3]. Different techniques to fabricate metallic nanoparticles on semiconductor substrates for SERS applications have been reported. For example, Kao *et al.* demonstrated a controllable uniform SERS substrate with metalized nanostructured poly (p-xylylene) films [4]. Qiu *et al.* fabricated silver-capped silicon nanowires using an electroless metal deposition method to achieve high SERS intensities [5]. Chan *et al.* demonstrated a porous silicon SERS substrate for small molecules by using a 6-step fabrication method [6]. Lin *et al.* developed a method to fabricate silicon wafer SERS substrates in the aqueous solution of silver nitrate machined by the fs laser [7]. Diebold *et al.* employed the fs laser pulse-train to fabricate a nanostructured silicon substrate followed by silver thermal evaporation for SERS detections [8].

In this paper, we report a simple method that can simultaneously fabricate nanostructures and generate silver nanoparticles by fs laser pulses over a large area of the silicon substrate. The SERS substrate was measured to have higher than 5×10^5 of EF using R6G as the analyte molecule at the excitation wavelength of 632.8 nm. This technique shows a possibility of integrating SERS capability to high order microdevice systems for chemical or biological detections.

2 Experiment

The SERS substrate is prepared in the following steps. First, a silicon wafer sample was cleaned ultrasonically in methanol and then dipped into a 1.0 M aqueous silver nitrate solution for 10 min at room temperature. Next, the sample was removed from the silver nitrate solution and air dried [9]. A thin layer of silver nitrate was formed on the sample surface. Finally, the silicon sample was processed by the fs laser micromachining system. The repetition rate, center wavelength and pulse width of the fs laser (Legend-F, Coherent, Inc.) are, respectively, 1 kHz, 800 nm and 120 fs. The laser fluence can be adjusted by a combination of a half-wave plate and a linear polarizer and the laser light was directed into an objective lens (Olympus UMPLFL 20×, NA=0.46) and focused onto the upper surface of the silicon sample. The silicon sample was moved by a computer controlled stage at the desired speed. Upon finishing a line scan, the silicon sample was stepped transversely by 2 μm to start another line scan. It took about 2 min to complete a 200 μm × 60 μm area. After fs laser micromachining, the silicon sample was rinsed with acetone to remove extra silver nitrate. The sample was dried by N_2 flow and was immediately used for SERS measurements to avoid surface oxidation in air.

Characterization of the silicon SERS substrate was carried out on a Raman spectroscopy system (Horiba Jobin Yvon). A 632.8 nm He–Ne laser was used to excite the Raman signal. Raman spectra were recorded through a 10× microscope objective (NA=0.25) and projected onto a charge-coupled device (CCD) array using a 600 line/mm grating with an integration time of 2 s.

3 Results and discussion

Figure 1 shows the field emission scanning electron microscope (SEM) images of the fs laser nanostructured silicon substrate. The thickness of the silver nitrate coating is about 700 nm, Fig. 1(a). The laser machining direction is from left to right, and the periodic structures can be clearly seen on the machined silicon substrate, Fig. 1(b), which has been reported [10, 11]. From the high magnification SEM image, Fig. 1(c), many nanoparticles in the size of 20–100 nm were found on the laser ablated silicon substrate. Those silver nanoparticles were confirmed and proved by EDS (Energy-dispersive X-ray spectroscopy) results which are not shown here. And for comparison purposes, a silicon substrate without coating with a silver nitrate solution was machined under the same conditions, and there are no nanoparticles on the nanostructures, Fig. 1(d).

The spectra of the laser ablated silicon substrates were measured as shown in Fig. 2. Trace (a) is the SERS spectrum of the R6G solution (10^{-6} M) on a randomly selected spot in the laser ablated area with the excitation laser power of 1.7 mW and integration time of 2 s. Trace (b) is the Raman spectrum of the R6G solution of 10^{-3} M concentration measured on the ablated silicon substrate without $AgNO_3$ coating using the excitation laser power of 8.5 mW and integration time of 2 s. Trace (c) is the Raman spectrum of the R6G solution of 10^{-3} M concentration measured on the unablated silicon substrate with $AgNO_3$ coating using the excitation laser power of 8.5 mW and integration time of 2 s. The trace (a) peak positions are listed in Table 1. By comparing traces (a) and (b), it clearly indicates the strong SERS spectrum in trace (a) is caused by the existence of silver nanoparticles due to the photoreduction of $AgNO_3$, and the nanostructures alone caused by fs laser micromachining have no effect on SERS. Without fs laser

micromachining, there is no SERS signal for a substrate coated with a silver nitrate layer. The Raman scattering cross-section EF can be estimated by the following equation [12, 13]

$$EF = \frac{I_{SERS} N_{nR}}{I_{nR} N_{SERS}} \quad (1)$$

where I_{nR} and I_{SERS} are, respectively, the normal Raman and SERS intensities in the unit of $mW^{-1}sec^{-1}$ [14]. N_{nR} and N_{SERS} represent, respectively, the number of molecules probed on the reference sample and on the SERS substrate. Using the Raman peak at 610 cm^{-1} as the basis of calculation [15], the EF was estimated to be 5.4×10^5.

The XPS (X-ray Photoelectron Spectroscopy, KRATOS AXIS 165) measurements were conducted to verify the existence of silver particles. The sputter etching technique was performed to remove possible contaminations on the substrate. The full graph XPS spectra of the silicon SERS substrate are shown in Fig. 3(a). The C_{1s} peak at the binding energy of 284.5 eV (NIST X-ray Photoelectron Spectroscopy Database) was used as an energy reference. As seen in Fig. 3(b), the peak value of C_{1s} is 285.0 eV, which implies the standard correction factor of C_{1s} is 0.5 eV (charge-shift value). Hence, the true value of Ag_{3d} should be 368.1 eV (i.e., 368.6 – 0.5), Fig. 3(c), which is consistent with the standard value of 368.2 eV for Ag^0. Hence, we can conclude that the Ag^+ ions have been reduced to Ag^0 atoms.

Parametric studies were also conducted to study the effect of two major process parameters on the intensity of SERS. Figure 4 shows the effect of laser scan speed on the SERS enhancement factor at the laser fluence of 3.56 J/cm^2. It is clearly seen that there is a peak and the EF rapidly decreases to very low values when the scan speed is higher

than about 18 mm/min. At a high laser scan speed, for a given laser fluence, the substrate cannot be ablated to form nanostructures, and there is no time for photoreduction to produce silver nanoparticles. On the other hand, at a very low laser scan speed, most of the silver nitrate coating is ablated and removed and very few silver nanoparticles remain. Figure 5 shows the EF increases as the laser fluence increases at the scan speed of 10 mm/min. The EF reaches the maximum at the laser fluence of about 3.56 J/cm^2 and then it decreases as laser fluence increases. It is interesting to note that even at very high laser fluences, the EF is low but not zero. This indicates that even at a very high laser fluence, not all silver nitrate coating is ablated away by laser pulses. This is in contrast to the results shown in Fig. 4 in which when the laser scan speed is too high, there is no SERS spectrum because the silver nitrite cannot be photoreduced to become silver nanoparticles.

Due to the multiphoton effect of the fs laser pulses, silver nitrate is ionized to become silver ions which are then reduced to silver nanoparticles through the following process: $2AgNO_3 \rightarrow 2Ag + 2NO_2\uparrow + O_2\uparrow$. However, the photoreduction can occur only when laser energy exceeds a threshold value and lasts a certain period of time which allows the photoreduction to act. In this study, as the silver nitrate is pre-coated on the substrate, a high laser intensity may remove the coating leading to no or very few silver nanoparticles. Hence, in order to achieve the maximum SERS spectra, several competing factors need to be considered in the laser micromachining process. After ultrasonical methanol bathing of the SERS substrate, the SERS spectra, although a little weaker, still exist. Hence, the fs laser pulses not only can reduce the silver ions, but can also fuse the

silver particles onto the silicon substrate [10], which may enhance the stability and reliability of the SERS substrate.

4 Conclusion

In summary, we present a simple method to simultaneously obtain nanostructures and silver nanoparticles on the surface of the silicon substrate by using fs laser pulses for SERS applications. An EF of 5.4×10^5 was achieved. The proposed fast fabrication method for SERS has potential applications for biological or chemical detections.

Acknowledgment This paper was partially supported by the Intelligent Systems Center, Missouri S&T.

References

1. M. Fleischmann, P.J. Hendra, and A.J. Mcquillan, Chem. Phys. Lett. 26, 163 (1974)
2. D.L. Jeanmaire and R.P. Van Duyne,J. Electroanal. Chem. 84, 1 (1977).
3. S. Nie and S. R. Emory, Science 275, 1102 (1997)
4. P. Kao, N.A. Malvadkar, M. Cetinkaya, H. Wang, D.L. Allara, and M.C. Demirel, Adv. Mater. 20, 3562 (2008)
5. T. Qiu, X.L. Wu, J. C. Shen, C. T. Ha, and K. Chu, Nanotechnology 17, 5769 (2006)
6. S. Chan, S. Kwon, T. Koo, L. Lee, and A. Berlin, Adv. Mater. 15, 1595 (2003)
7. C. Lin, L. Jiang, Y. Chai, H. Xiao, S. Chen, and H.L. Tsai, Opt. Express 17, 21581 (2009)
8. E. Diebold, N. Mack, S. Doorn, and E. Mazur, Langmuir 25, 1790 (2009)
9. J. Xu, Y. Liao, H. Zeng, Z. Zhou, H. Sun, J. Song, S. Wang, Y. Cheng, Z. Xu, K. Sugioka, and K. Midorikawa, Opt. Express 15, 12743 (2007)
10. C. Wu, C. Crouch, L. Zhao, and E. Mazur, Appl. Phys. Lett. 81, 1999 (2002)
11. Y. Han, C. Lin, H. Xiao, and H.L. Tsai, Microsys. Technol. 15, 1045 (2009)
12. A. Kudelski, Phys. Lett. 414, 271 (2005)
13. H.K. Park, J.K. Yoon, and K. Kim, Langmuir 22, 1626 (2006)
14. R.P. Van Duyne, J.C. Hulteen, and D.A. Treichel, J. Chem. Phys. 99, 2101 (1993)
15. S. Santesson, J. Johansson, L.S. Taylor, I. Levander, S. Fox, M. Sepaniak, and S. Nilsson, Analytical Chem. 75, 2177 (2003)

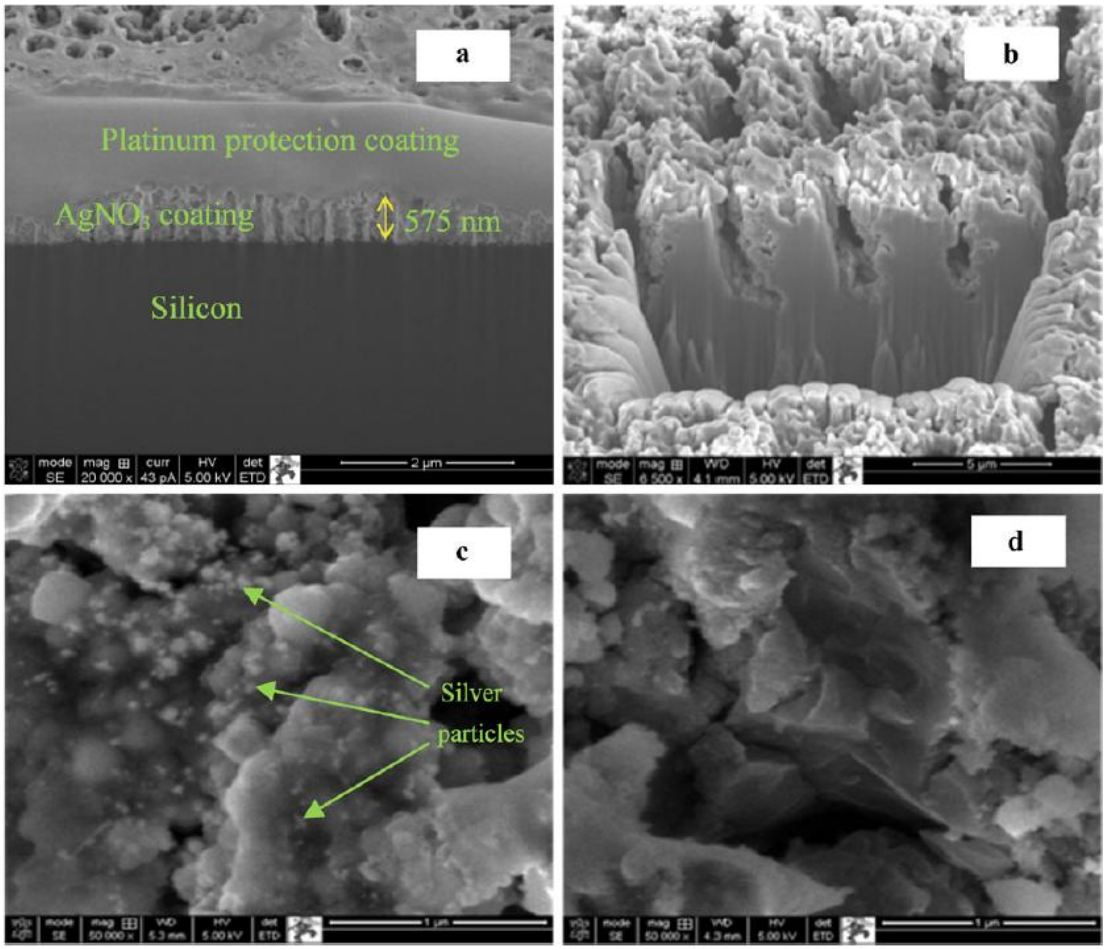

Fig. 1 (a) SEM image showing the thickness of $AgNO_3$ coating (tilted 45 degrees), (b) SEM image showing the surface substructure after fs laser micromachining, (c) high magnification of the SEM image showing silver nanoparticles on laser machined substrate with $AgNO_3$ coating, (d) high magnification of the SEM image showing no silver nanoparticles on laser machined substrate without $AgNO_3$ coating

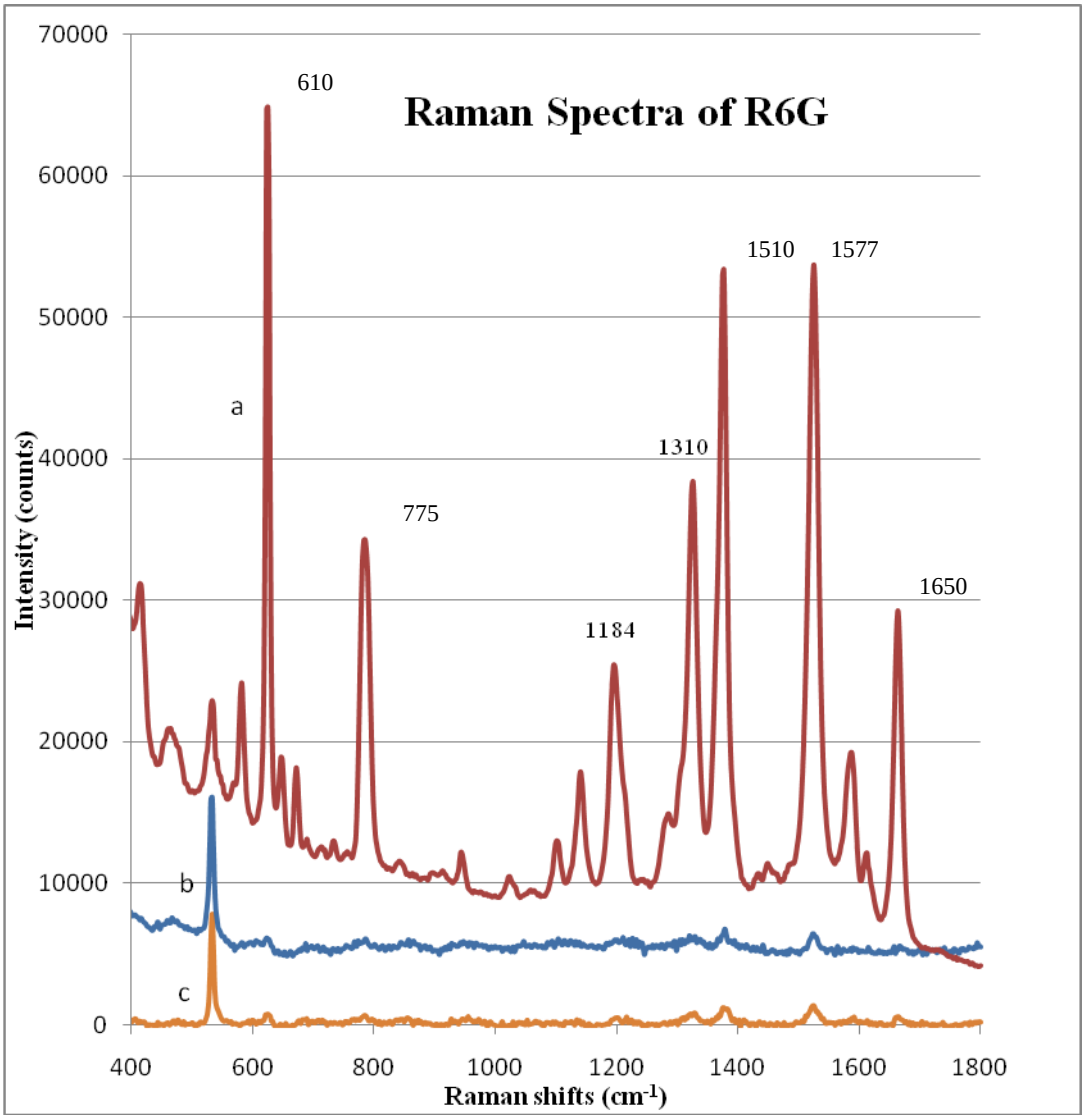

Fig. 2 (a) SERS spectrum of R6G 10^{-6} M solution on the laser ablated SERS silicon substrate with an excitation laser power of 1.7 mW and integration time of 2 s, (b) Raman spectrum of R6G 10^{-3} M solution on the laser ablated silicon substrate without $AgNO_3$ coating with an excitation power of 8.5 mW and integration time of 2 s, (c) Raman spectrum of R6G 10^{-3} M solution on the unablated silicon substrate with $AgNO_3$ coating with an excitation power of 8.5 mW and integration time of 2 s

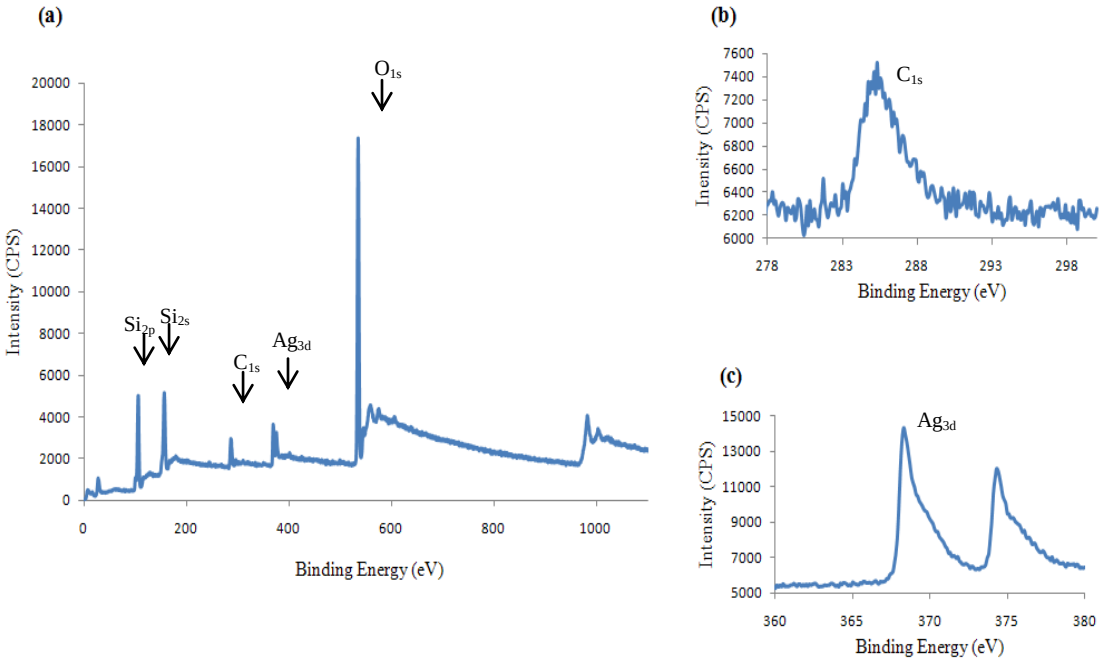

Fig. 3 XPS graph of the silicon SERS substrate. (a) full graph (1000 ms per 1 eV); (b) graph of C_{1s} (500 ms per 0.1 eV); (c) graph of Ag_{3d} (500 ms per 0.1 eV)

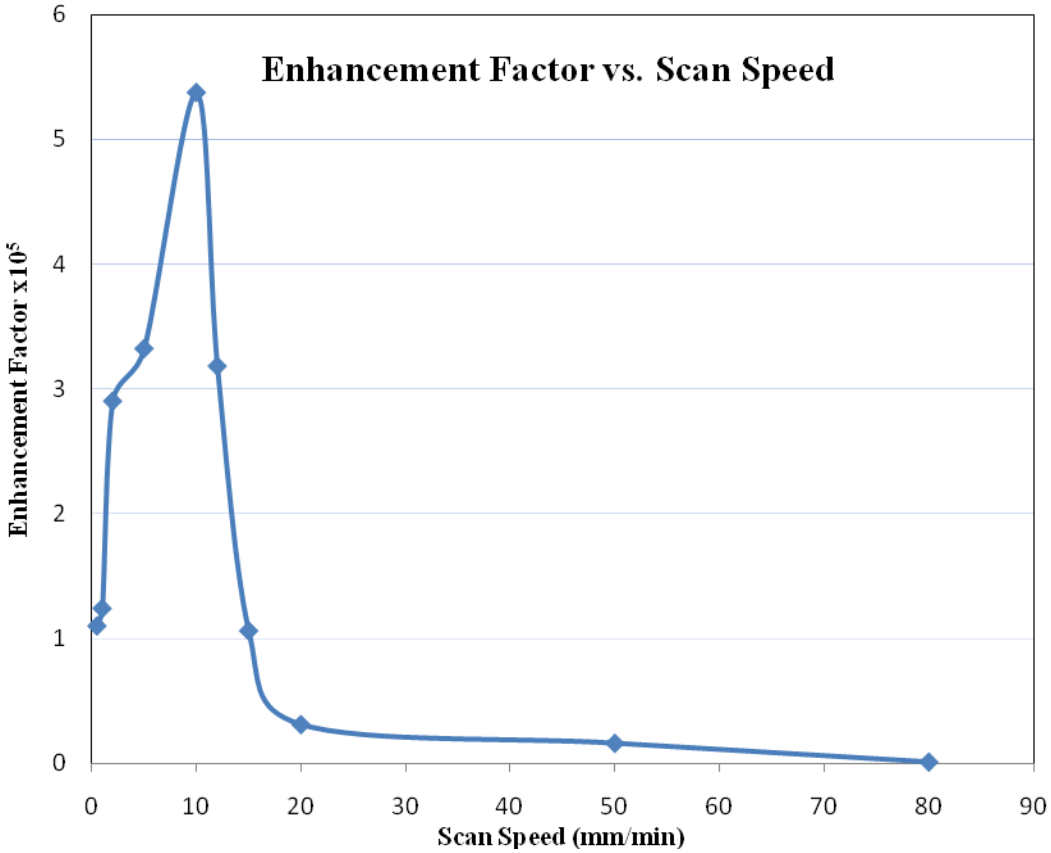

Fig. 4 SERS enhancement factor vs. scan speed; laser fluence is 3.56 J/cm^2

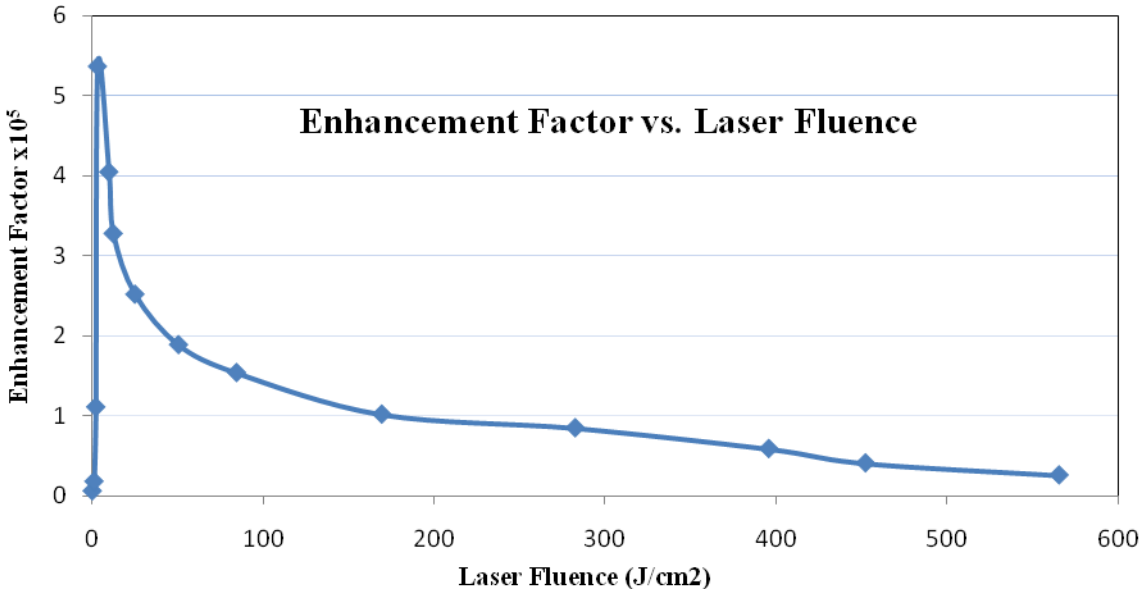

Fig. 5 SERS enhancement factor vs. laser fluence; scan speed is 10 mm/min

Table 1 Peak positions of R6G on the silicon SERS substrate

Assignment	Raman shifts (cm^{-1})
Xanthenes ring deformations	610
C-H bend	775
Xanthenes ring deformations , C-H bend, N-H bend	1184
Xanthenes ring deformations , N-H bend, CH_2 wag	1310
Xanthenes ring deformations , C-H bend	1360
Xanthenes ring deformations, C-N stretch, C-H bend, N-H bend	1510
Xanthenes ring deformations, N-H bend	1577
Xanthenes ring deformations, C-H bend	1650

SECTION

2. CONCLUSIONS

It is shown in this dissertation that femtoscond laser micromachining is a good method to fabricate 3D microstructures on fused silica and silicon. A clean, high quality surface was achieved on the silicon wafer under some specific laser machining parameters in the water confinement. It is unique way to avoid periodic structures that is induced by the femtosecond laser machining in the air on the machined silicon surface. It can help improve the silicon machining quality in many applications. A fiber inline IFPI based measurement method was used to investigate the fs laser induced refractive index change in optical fiber core. The fs laser induced refractive index change was found out as 2.5×10^{-6}, 2.78×10^{-5}, 3.45×10^{-4} and 8.95×10^{-4} at different pulse energy levels, 0.5 μJ, 0.6 μJ, 0.8 μJ and 1 μJ, respectively. A SERS substrate fabricated by femtosecond laser ablation on a silica glass, followed by chemical plating of silver, was demonstrated. An EF of 2.5×10^{6} was measured using a 10^{-7} M R6G solution. Besides the high EF, the femtoseond laser structured area has shown a good uniformity characterized by Raman mapping. A simple method was developed to simultaneously obtain nanostructures and silver nanoparticles on the surface of the silicon substrate by using femtosecond laser pulses for SERS applications. An EF of 5.4×10^{5} was achieved. The proposed fast fabrication method for SERS has potential applications for biological or chemical detections.

BIBLIOGRAPHY

[1] D. Villar, I. R. Matias, and F. J. Arregui, "Enhancement of sensitivity in long- period fiber gratings withdeposition of low-refractive-index materials," Opt. Lett. 30, 2363-2365 (2005).

[2] W. Liang, Y. Huang, Y. Xu, R. K. Lee, and A. Yariv, "Highly sensitive fiber Bragg grating refractive index sensors," Appl. Phys. Lett. 86, 151122:1-3 (2005).

[3] I. M. White, H. Oveys, and X. Fan, "Liquid-core optical ring-resonator sensors," Opt. Lett. 31, 1319-1321 (2006).

[4] B. Gauvreau, A. Hassani, M. Fassi Fehri, A. Kabashin, and M. A. Skorobogatiy, "Photonic bandgap fiberbased Surface Plasmon Resonance sensors," Opt. Express 15, 11413-11426 (2007).

[5] N. Skivesen, A. Tetu, M. Kristensen, J. Kjems, L. H. Frandsen, and P. I. Borel, "Photonic-crystal waveguide biosensor," Opt. Express 15, 3169-3176 (2007).

[6] I. M. White and X. Fan, "On the performance quantification of resonant refractive index sensors," Opt. Express 16, 1020-1028 (2008).

[7] Y. J. Rao, "Recent progress in fiber-optic extrinsic Fabry-Perot interferometric sensors," Opt. Fiber Technol. 12, 227-237 (2006).

[8] V. Bhatia, K. A. Murphy, R. O. Claus, M. E. Jones, J. L. Grace, T. A. Tran, and J. A. Greene, "Optical fiber based absolute extrinsic Fabry - Perot interferometric sensing system," Meas. Sci. Technol. 7, 58-61 (1996).

[9] H. Xiao, J. Deng, G. Pickrell, R. G. May, and A. Wang, "Single-crystal sapphire fiber-based strain sensor for high-temperature applications," J. Lightwave Technol. 21, 2276-2283 (2003).

[10] Y. Zhang, X. Chen, Y. Wang, K. L. Cooper, and A. Wang, "Microgap Multicavity Fabry–Pérot Biosensor," J. Lightwave Technol. 25, 1797-1804 (2007).

[11] G. Z. Xiao, A. Adnet, Z. Y. Zhang, F. G. Sun, and C. P. Grover, "Monitoring changes in the refractive index of gases by means of a fiber optic Fabry-Perot interferometer sensor," Sensor Actuat. A-Phys. 118, 177-182 (2005).

[12] Z. L. Ran, Y. J. Rao, W. J. Liu, X. Liao, and K. S. Chiang, "Laser-micromachined Fabry-Perot optical fiber tip sensor for high-resolution temperature-independent measurement of refractive index," Opt. Express 16, 2252-2263 (2008).

[13] Y. J. Rao, M. Deng, D. W. Duan, X. C. Yang, T. Zhu, and G. H. Cheng, "Micro Fabry-Perot interferometers in silica fibers machined by femtosecond laser," Opt. Express 15, 14123-14128 (2007).

[14] Z. L. Ran, Y. J. Rao, H. Y. Deng, and X. Liao, "Miniature in-line photonic crystal fiber etalon fabricated by 157 nm laser micromachining," Opt. Lett. 32, 3071-3073 (2007).

[15] T. Vo-Dinh, "Surface-enhanced Raman spectroscopy using metallic nanostructures," Trac-Trend Anal. Chem. 17, 557-582 (1998).

[16] C. Gu and C. Shi, "Fiber-based sensors: surface-enhanced Raman sensors improve detection of dangerous agents," Laser Focus World. 45, 97 (2009).

[17] C. Viets, W. Hill, "Comparison of fibre-optic SERS sensors with differently prepared tips," Sens. Actuators B 51, 92-99 (1998).

[18] D. L. Stokes and T Vo-Dinh, "Development of an integrated single-fiber SERS sensor," Sens. Actuators B 69, 28-36 (2000).

[19] A. Lucotti and G. Zerbi, "Fiber-optic SERS sensor with optimized geometry," Sens. Actuators B 121, 356-364 (2007).

[20] C. Viets and W. Hill, "Laser Power Effects in SERS Spectroscopy at Thin Metal Films," J. Phys. Chem. B 105, 6330-6336 (2001).

[21] H. Yan, J. Liu, C. Yang, G. Jin, C. Gu and L. Hou, "Novel index-guided photonic crystal fiber surface-enhanced Raman scattering probe," Opt. Express 16, 8300-8305 (2008).

VITA

Yukun Han was born on August 01, 1980 in Puyang, Henan, China. She received her secondary education in Puyang, graduating from Puyang High School in July of 1998. In June 2002, she received her B.S. in Material Science and Engineering from Shanghai Jiaotong University, Shanghai, China.

In March 2005, she received her M.S. in Material Processing Engineering from Shanghai Jiaotong University, Shanghai, China.

Yukun Han won the 3rd place award for the poster titled "Femtosecond laser one-step fabrication of microstructures for sensing and detection" at the fifth annual Intelligent Systems Center poster presentation on November 11, 2009 at Missouri University of Science and Technology.

In May 2011, she received her Ph. D. under the guidance of Dr. Hai-Lung Tsai in Mechanical Engineering from Missouri University of Science and Technology, Rolla, Missouri, USA.

During her graduate study, she authored and co-authored 8 journal papers and 6 conference papers.